



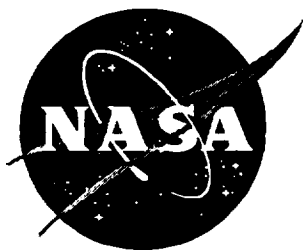
NASA Contractor Report 4748

Integrated Control Using the SOFFT Control Structure

Nesim Halyo

Contract NAS1-20185
Prepared for Langley Research Center

July 1996



Integrated Control Using the SOFFT Control Structure

Nesim Haljo

Information & Control Systems, Inc. • Newport News, Virginia

Printed copies available from the following:

NASA Center for AeroSpace Information
800 Elkridge Landing Road
Linthicum Heights, MD 21090-2934
(301) 621-0390

National Technical Information Service (NTIS)
5285 Port Royal Road
Springfield, VA 22161-2171
(703) 487-4650

FOREWORD

The work described in this report was performed by Information & Control Systems, Incorporated (ICS) under NASA Contract Number NAS1-20185 for the National Aeronautics and Space Administration (NASA), Langley Research Center (LaRC). The work was sponsored under the Small Business Innovation Research (SBIR) program.

Mr. Aaron Ostroff was the NASA Technical Representative for this contract. Dr. Nesim Halyo was the ICS project manager.

All the design, analysis and simulation results shown in this report were obtained using our Computer-Aided Control System Design (CACSD) software package ACETTM.

We would like to acknowledge Mr. Aaron Ostroff for many insightful discussions on the Integrated SOFFT Control methodology developed during this contract. We would like to thank National Aeronautics and Space Administration for its support of this important work.

TABLE OF CONTENTS

FOREWORD	iii
LIST OF FIGURES	vi
LIST OF TABLES	vii
I. INTRODUCTION	1
Why Use Integrated Control	2
Summary	3
II. INTEGRATED SOFFT CONTROL	5
A. CENTRALIZED SOFFT CONTROL	5
1. Problem Formulation	7
Feedforward Control	8
Feedback Control	11
2. The SOFFT Control Structure	15
B. INTEGRATED SOFFT CONTROL:	
A NEW APPROACH	18
1. Problem Formulation	20
2. A SOFFT Approach To Integrated Control	22
Coupling as Disturbance	23
Centralized or Integrated	24
Different Strokes	25
C. INTEGRATED FEEDFORWARD CONSIDERATIONS	28
1. Control-Dependent Measurements	29
2. Unstable Open-loop Plant	31

TABLE OF CONTENTS (CONTINUED)

III. INTEGRATED/CONSTRAINED OUTPUT FEEDBACK	
CONTROL	33
A. TIME-INVARIANT PROBLEM FORMULATION	33
B. ALGORITHM DEVELOPMENT	39
1. Necessary Conditions	39
2. Constrained Algorithm	41
C. EXTENSION TO VARIABLE-GAIN SYSTEMS	44
Integrated/Constrained Variable-Gain	
Feedback Algorithm	47
IV. AN INTEGRATED FLIGHT AND PROPULSION	
CONTROL EXAMPLE	51
A. AIRFRAME AND PROPULSION MODELS	51
B. FEEDFORWARD CONTROL DEVELOPMENT	57
1. Input Command Considerations	58
2. Command Model or Flying Qualities	60
3. Feedforward Control Gain Matrices	62
C. FEEDBACK CONTROL DEVELOPMENT	65
1. Feedback Constraints	66
2. Feedback Gain Matrix	67
D. SIMULATION RESULTS	69
V. CONCLUSIONS	82
REFERENCES	84
APPENDIX A	86
APPENDIX B	89

LIST OF FIGURES

Figure 1. Typical Error Feedback Control Law	6
Figure 2. SOFFT Control Structure	15
Figure 3. SOFFT Control Law Structure	16
Figure 4. Modified F-15 SMTD Integrated SOFFT Control	
Simulation, $\alpha = 30^\circ$	
a. Pilot Input Commands	70
b. Command Model Outputs	71
c. Airframe Variables	72
d. Propulsion Variables	73
e. Control Variables	74
Figure 5. Modified F-15 SMTD Integrated SOFFT Control ,	
Perturbed Plant	
a. Pilot Input Commands	75
b. Command Model Outputs	76
c. Airframe Variables	77
d. Propulsion Variables	78
e. Feedforward Control Variables	79
f. Feedback Control Variables	80

LIST OF TABLES

Table 1. Airframe Controls	52
Table 2. Airframe State Variables	53
Table 3. Propulsion Control Variables	53
Table 4. Propulsion State Variables	54
Table 5. Integrated System A_x Matrix	55
Table 6. Integrated System B_x Matrix	56
Table 7. Integrated System Measurement/Feedback Variables	57
Table 8. Integrated System Modified B_x Matrix	61
Table 9. Feedforward Control Gain Matrix : K_x^*	63
Table 10. Feedforward Control Gain Matrix : K_z	63
Table 11. Feedforward Control Gain Matrix : K_w	63
Table 12. Constraint (Zero) Matrix : Z	67
Table 13. Constrained Feedback Gain Matrix : K	68
Table 14. Unconstrained Feedback Gain Matrix : K	69
Table 15. Closed Loop Equivalent s-plane Eigenvalues	81

I. INTRODUCTION

The recent trend toward enhancing the overall maneuvering capabilities of aircraft has resulted in the development of new advanced aircraft such as the Short Take-Off Vertical Landing (STOVL) and, more recently, the X-36 Tailless Fighter among others. This trend has also produced new and enhanced subsystems, such as advanced propulsion subsystems with vectored thrust, which must be closely coordinated or integrated with the existing aircraft subsystems, such as the aerodynamic airframe subsystems which may now have unconventional aerodynamic control surfaces. The potential capabilities of the resulting aircraft have significantly improved. However, **to achieve this potential, we must face the challenge of integrating all the aircraft subsystems so that each subsystem cooperates with the others in a way that enhances or optimizes the overall capabilities of the aircraft.** IMPACT or Integrated Methodologies for Propulsion and Airframe Control Technologies is a program that addresses these design concerns.

In this work, we will develop a new methodology for designing an integrated control system which produces coordinated action among the subsystems while limiting the complexity of the control law and maintaining the identity of the subsystems in the closed-loop system. To achieve these objectives, we will use the SOFFT or Stochastic Optimal Feedforward and Feedback Technology structure [1] for the control system. We will modify and extend the SOFFT methodology as needed so as to produce the desired level of integration and cooperation among the subsystems. Building upon previously developed methods such as those described in [2]-[10], we will also develop a feedback control algorithm which limits feedback between specified subsystem variables so as to maintain the identity of the desired subsystems while allowing feedback communication among others to obtain the desired level of cooperation among them. We will apply the methodology developed to the design of an integrated flight and propulsion control system for a modified F-15 SMTD aircraft to provide an example of the design methodology.

At present, the usual approach in designing control laws for complex systems which contain some degree of coupling among several subsystems is to design independent control laws for each subsystem, then try to produce some integration by an outer loop design between selected subsystems, while others are left separate or uncoupled. An example of these approaches is found in designing the longitudinal and lateral flight control systems for most aircraft. The longitudinal and lateral dynamics are not coupled in level flight, but become coupled as soon as the aircraft rolls and has a nonzero bank angle. However, the longitudinal and lateral flight control laws are usually designed independently, without any coupling, and are usually left uncoupled. In the case of the propulsion system, the longitudinal and propulsion control systems are usually designed independently. Often, the two subsystem designs are left uncoupled with the thrust as the propulsive subsystem command while the pitch rate or other suitable variable is the longitudinal airframe subsystem command. Sometimes, an autothrottle system is designed which then couples the two closed-loop subsystems. In both cases, the original design of the subsystem control laws is done with no cross-coupling or cross-communication among the subsystems.

Why Use Integrated Control?

When the subsystems have no coupling, using a control law with cross-coupling does not improve performance, at least when a quadratic objective function is being used. On the other hand, when the subsystems are coupled to some degree, the optimal feedback control law will contain nonzero cross-coupling terms. In this case, **designing the control law for each subsystem independently from the others corresponds to treating any coupling terms from the other subsystems as unknown disturbances.** Then, each subsystem control law must be designed to worst case specifications as if the disturbances were of an unknown nature. While performing a maneuver, the coupling from the other subsystems would have to build up into noticeable errors in the controlled variables, beyond the level of error usually caused by sensor noises and other truly random disturbances, before the control law can even start to take corrective action to reduce the error. On the other hand, knowing the dynamics of the coupling terms, a centralized/coupled control system can act before errors due to the coupling terms build up, thus producing a better performance.

While a completely coupled or centralized control law may produce less error in performing maneuvers, it also has some disadvantages. A completely coupled or centralized control law would feed every subsystem state variable (or every sensor measurement in the output feedback case) to every subsystem control variable. This usually results in a very complicated and impractical control law. State variables which have minimal effect on a subsystem end up being fed into the subsystem for reasons which are difficult to understand. In general, the complexity of the control law and the closed-loop system make it difficult to understand and hard to analyze, particularly in evaluating nonlinear effects.

Another important disadvantage of a centralized or fully coupled control law is the subsystems can lose their identity within the closed-loop system. When each state variable is fed into each subsystem, the original properties of the subsystem become theoretically less meaningful. Independent system validation is no longer meaningful. However, from a practical standpoint, analysis of each subsystem and validation of its operation under various circumstances is a necessary part of the flight procedure.

Thus, the best solution to the question of integrating subsystems is a compromise in which some state variables or sensor measurements are fed into certain subsystems which may be specified by the control system designer while other states or measurements are only fed into the subsystem from which they originated but are not allowed into the remaining subsystems. Each subsystem control law feeds back its own states or measurements plus a limited number of variables which couple it to the other subsystems. The selection of the constraints and the corresponding selection of the control law structure is left to the control system designer who can take advantage of the specific system requirements for each design problem.

Summary

In Section II, we will first summarize the SOFFT control methodology developed previously for the centralized case. Then, we will describe the approach of using the feedforward control law in a different way than the feedback control law for purposes of integration. Finally, we will consider the impact of specific problems, such as an unstable open-loop plant and control -dependent measurements, on the design of the integrated feedforward SOFFT control law.

In Section III, we will consider the feedback control law. We will formulate the sampled-data stochastic output feedback problem with constraints among the subsystems for a single model or for a time-invariant linear system. We will develop an algorithm to compute the feedback control gain matrix with the given constraints. Then, we will extend the problem to the Variable-Gain case. Finally, we will consider some other applications of the constrained output feedback problem which may be of interest.

In Section IV, we will apply the methodology developed in the previous sections to the design of an integrated flight and propulsion control system for the modified F-15 SMTD aircraft at one flight condition. We will describe the selection of the command model to produce the desired flying qualities, the selection of the feedback control structure and the results of a linear simulation.

Our main conclusion is that our approach of using a SOFFT structure with a centralized/coupled feedforward control law and a constrained output feedback control law provides an excellent solution to the problems associated with Integrated Control.

II. INTEGRATED SOFFT CONTROL

The approach of designing the subsystem control laws independently from each other, thus having an uncoupled control law, can be improved by including some level of integration into the design. On the other hand, a completely centralized control law (e.g., a full state feedback control law) for the overall integrated system has the disadvantages described in the Introduction; namely, increased complexity and the loss of subsystem identity. Therefore, the best approach to integrated control design is to allow coupling or communication among the subsystems where improvement of the overall performance is possible, but limit the coupling among the subsystems where this will lead to increased complexity and not much improvement in the performance.

The SOFFT control structure developed in [1] provides an excellent vehicle for achieving these objectives: limit complexity, maintain subsystem identity, yet provide coupling where performance improvement is possible. For ease of understanding and for completeness, we will first provide a short summary of the SOFFT control approach for centralized systems. Then, we will describe how we can extend this approach to develop an Integrated Control design methodology while still maintaining the important advantages of the SOFFT control approach itself. Finally, we will consider some special problems which are of interest in designing integrated control systems.

A. CENTRALIZED SOFFT CONTROL

The Stochastic Optimal Feedforward and Feedback Technique (SOFFT) is a control design methodology in which the feedback and feedforward control laws are designed separately, each using optimal control, and are combined using the SOFFT control structure which results from the problem formulation[1], [2]. Many control systems are designed essentially as feedback control laws, sometimes preceded by a shaping filter as

shown in Figure 1. One of the main motivations of the SOFFT approach has been the observation that a feedback system is inherently a reactive controller. In other words,

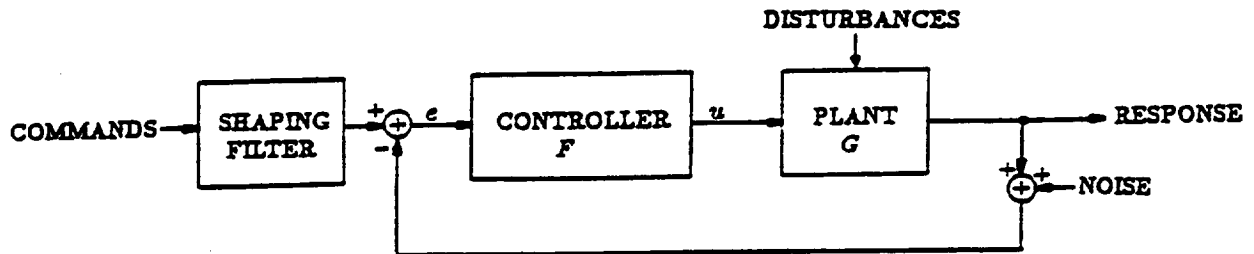


Figure 1. Typical Error Feedback Control Law

a feedback system only reacts to errors after they have occurred. A feedback control system produces no control command when the state has no current errors even if the (pilot) input commands are nonzero.

To produce the desired response to input commands, such as flying qualities, it is necessary to use a feedforward control law in some way. The explicit model following problem defines an optimal control problem with a cost function which penalizes deviations from a given command model trajectory and also penalizes control activity. The explicit model follower contains both a feedforward and a feedback control law and solves the problem of the feedback control law being only reactive. The explicit model follower produces nonzero commands even when the state error is zero if the input commands are nonzero. In this control law, the feedback and feedforward control laws (i.e., the corresponding gain matrices) are highly dependent on each other because they are obtained by optimizing a single cost function.

The basic problem with the explicit model following formulation is that it combines the command tracking objectives (tracking errors) with the objectives of noise attenuation and robustness into a single cost function. The result is that an explicit model follower cannot follow an arbitrary command without some tracking error even when the system model is known perfectly and there are no random noises or disturbances.. This is due to the fact

that any nonzero command requires some nonzero control action. But since control action is penalized to achieve the usual feedback objectives, the optimal control does not produce zero tracking error, but a combination of some tracking error and control activity which results in a lower cost. On the other hand, if we do not penalize control action, the resulting control will respond to any noise or random disturbance thus possibly amplifying noise rather than attenuating it. Thus, the explicit model following problem places conflicting demands on the problem. In general, to produce better command tracking, we have to give up noise attenuation or robustness.

The SOFFT formulation provides a solution to these problems by separating the objectives for the feedforward control from those related to the feedback control. Accordingly, it becomes possible to track input commands perfectly, with zero error, when the system model is known perfectly and no random noises are present. This command tracking objective is achieved without a corresponding deterioration in the feedback control objectives such as noise attenuation, random disturbance accommodation or system stability.

In the SOFFT approach, we consider command tracking or producing a desired response to given (pilot) input commands as a feedforward control objective. On the other hand, noise attenuation, disturbance accommodation and stability are considered to be feedback control objectives. In other words, we do not attempt to produce flying qualities with the feedback control law, just as we would not try achieve system stability with the feedforward control law.

1. Problem Formulation

Consider the linear system defined in (1) and (2).

$$x_{k+1} = \Phi_x x_k + \Gamma_x u_{xk} + w_{xk} \quad (1)$$

$$y_{xk} = C_x x_k + v_{xk} \quad (2)$$

where x_k is the n_x -dimensional state vector, u_{xk} is the n_{ux} -dimensional control vector, y_{xk} is the n_{yx} -dimensional measurement or feedback vector, w_{xk} and v_{xk} are the plant and

measurement noise vectors, respectively. We assume that the plant and measurement vectors are zero mean white noise sequences uncorrelated to each other. We will consider the plant and measurement equations shown above to be sampled-data discretizations of a continuous time system such as airframe or propulsion dynamics systems. However, the development described here applies to a purely discrete system as well.

Note that the measurement or feedback vector in (2) does not depend on the control vector. We will extend the formulation to the case in which control-dependent measurements are present later in this section by embedding this case into the one shown in (2). However, here we will formulate the SOFFT problem for the plant and measurements shown above

Feedforward Control

Let us suppose that the plant control vector, u_{xx} , is composed of two parts: one part, u_{xx}^* , coming from the feedforward control law and the other part, \tilde{u}_{xx} , coming from the feedback control law. Thus,

$$u_{xx} = u_{xx}^* + \tilde{u}_{xx} \quad , \quad k = 0, 1, 2, \dots \quad (3)$$

Accordingly, part of the state and part of each measurement will be due to the feedforward control, u_{xx}^* , while the remaining portion will be produced by the feedback control, \tilde{u}_{xx} . The objective of the feedforward control law is to produce the control sequence which depends only on the pilot input commands (i.e., not on the noisy measurements which are fed back) and produces the desired system response when no random plant or measurement noise is present. Therefore, we define the feedforward state trajectory and measurements using the equations:

$$x_{k+1}^* = \Phi_x x_k^* + \Gamma_x u_{xx}^* \quad (4)$$

$$y_{xx}^* = C_x x_k^* \quad (5)$$

where the superscript "*" denotes the feedforward part of the variable with which it is used.

Now, consider a command model of the following form.

$$z_{k+1} = \Phi_z z_k + \Gamma_z u_{zk} \quad (6)$$

$$y_{zk} = H_z z_k \quad (7)$$

where the command model state, z_k , has n_z components which will usually be different, often much smaller, than plant state dimension, n_x . While other stochastic interpretations of the command model provide various possible applications ([1], pp. 17,18), here, we will only discuss one particular interpretation. We interpret the command input vector, u_{zk} , as the pilot command input vector; e.g., the pilot stick input. Furthermore, we will restrict the number of inputs to the command model (i.e., the dimension of u_{zk}) to be the same as the number of plant control components, n_{ux} . Therefore, the number of pilot input commands will be the same as the number of independent plant controls.

Now define the tracking error vector as follows.

$$e_k^* = H_y y_{zk}^* - H_z z_k \quad (8)$$

where the matrices H_y and H_z are selected by the control system designer so as to select the plant variables which should track the appropriate command model states. Here, we will assume that the dimension of the tracking error vector is the same as the number of input commands and the number of plant controls, n_{ux} .

If the tracking error is zero at every sampling instant, we have the "perfect tracking" case. Note that perfect tracking describes the feedforward trajectory only since the actual state will always have some tracking error due to sensor noise, plant noise, other disturbances and nonlinearities. If perfect tracking is not achieved for some reason, then we would want to minimize the tracking error using some optimization criterion as discussed in the following.

We select a cost function quadratic in the tracking error since the main purpose of the feedforward control law is to produce the specified response to the command model

inputs determined by (6), (7) and (8). To accommodate other possible objectives, we include other terms in the cost function.

$$J^* = \lim_{N \rightarrow \infty} \frac{1}{2(N+1)} E \left\{ \sum_{k=0}^N e_{k+1}^{*T} e_{k+1}^* + x_{k+1}^{*T} Q_1^* x_{k+1}^* + u_{xk}^{*T} R_1^* u_{xk}^* \right\} \quad (9)$$

where E denotes the expectation operator.

Since the pilot input commands are not known a priori, we model the u_{xk} as a stochastic process which we are measuring together with the other measurements. Here, we assume that we have a white noise process. Of course, it is possible to choose other statistics for this random process with minor modifications to problem formulation.

The SOFFT feedforward control is obtained as the solution of the following optimization problem. Find the control, u_{xk}^* , of the form

$$u_{xk}^* = -K_x^* x_k^* - K_z z_k - K_w u_{xk} \quad (10)$$

which minimizes the cost function (9) subject to the constraints (4) - (8).

The general solution to this problem is given in [2]. Here we will summarize the solution to the perfect tracking case. Observing the cost function (9), note that when the matrices Q_1^*, R_1^* vanish, the cost function is minimized if the tracking error is zero at every sampling instant. The only possible impediment to this would be the constraints (4) - (8). Thus, unless the system dynamics do not allow a particular trajectory, the optimal solution for this cost function would produce the perfect tracking feedforward control law.

For the perfect tracking case, the feedforward gain matrices are given by [2]

$$K_x^* = [H_x \Gamma_x]^{-1} H_x \Phi_x \quad (11)$$

$$K_z = -[H_x \Gamma_x]^{-1} H_z \Phi_z \quad (12)$$

$$K_{uz} = -[H_x \Gamma_x]^{-1} H_z \Gamma_z \quad (13)$$

where

$$H_x = H_y C_x \quad (14)$$

Thus, when the matrix $H_x \Gamma_x$ is non-singular, perfect tracking is possible and is given by the gain matrices above. When $H_x \Gamma_x$ is singular, there may be many solutions to the problem, so that adding further constraints may determine a unique solution. The more difficult case corresponding to a nearly singular matrix should be investigated in detail for the particular design problem under consideration. Generally, this implies that the control authority of the system may be insufficient to track certain trajectories commanded by the pilot. Alternately, it may also signal that the selected command vector is not suitable to the system being controlled.

It should be noted that the philosophy in perfect tracking is that the pilot knows the aircraft subsystems quite well and the command signals are not corrupted by random noise (since they are being computed by the on-board computer), so that the automatic control system tries to track his commands perfectly, if possible, unless constrained by the subsystems' physical limitations such as rate or position limits or other saturation processes.

Feedback Control

If the actual system contained no noise, had no disturbances, no limiters or other nonlinearities and the system parameters were known perfectly and did not vary, the feedforward control described above would be sufficient to control it. Of course, none of these conditions hold in practical situations. Accordingly, the basic objective of the feedback control law is to minimize any deviations from the commanded trajectory despite the presence of noises, disturbances, nonlinearities, parameter uncertainties, etc. A number of other objectives may be added to the list; e.g., type 1 behaviour in the commanded variables, reasonably low levels of control activity, etc.

Let us define the deviations or perturbations from the feedforward (or *) trajectory as follows.

$$\tilde{x}_k = x_k - x_k^* \quad (15)$$

$$\tilde{y}_{\text{xx}} = y_{\text{xx}} - y_{\text{xx}}^* \quad (16)$$

where the feedforward state and measurement vectors, x_k^* and y_{xx}^* respectively, are defined by (4) and (5). The perturbed control vector, \tilde{u}_{xx} , is similarly defined by (3).

Combining the plant equations (1) and (2) with the feedforward equations (4) and (5), we find that the perturbed variables are subject to the dynamical equations

$$\tilde{x}_{k+1} = \Phi_x \tilde{x}_k + \Gamma_x \tilde{u}_{\text{xx}} + w_{\text{xx}} \quad (17)$$

$$\tilde{y}_{\text{xx}} = C_x \tilde{x}_k + v_{\text{xx}} \quad (18)$$

In other words, the deviations in the state and measurements have the same dynamics as the original plant. It is important to note that the usual perturbation equations often used in such design problems describe the deviation of the total state variables from a fixed or constant operating point (or a nominal flight condition). The equations in (17) and (18), however, describe the deviation of the total state variables from the commanded trajectory which is not fixed, but may be performing a fast maneuver and transitioning from one operating point to another. A more detailed description of the derivation starting from the continuous nonlinear plant equations is given in [1].

While the feedforward control law may be performing a high agility maneuver, the objective of the feedback control law will be achieved by keeping the deviations described by (17) and (18) as small as possible despite all the noises and disturbances present in the system. If these deviations remain small, then the total state will be near the trajectory commanded by the pilot.

Here, we will consider a Proportional-Integral-Filter (PIF) feedback control structure as this versatile structure provides a type 1 control law with some smoothing (filter) to

reduce high frequency control activity which may result from random noises in the system. Almost any other structure can be used to produce other types of control laws [1].

To obtain a PIF control structure, augment the perturbation equations in(17) and (18) by the additional equations

$$\tilde{u}_{xk+1} = \tilde{u}_{xk} + \Delta t \tilde{v}_{xk} + w_{uk} \quad (19)$$

$$\tilde{I}_{k+1} = \tilde{I}_k + \Delta t (H_y \tilde{y}_{xk} + H_u \tilde{u}_{xk}) + w_{Ik} \quad (20)$$

where Δt is the sampling period used for digital control system, \tilde{v}_{xk} corresponds to the rate of change of the control position vector, \tilde{u}_{xk} , and \tilde{I}_k corresponds to the integrators of the perturbations or errors in the variables commanded by the feedforward control law. The noise terms have been added to the equations for generality. Since the computations corresponding to these equations will be performed on the control computer, there is no physical error that is introduced other than the round off occurring in the computations, generally a negligible term.

As a result of (19), note that the feedback control position, \tilde{u}_{xk} , has now become part of the augmented state vector and is no longer the control vector for the augmented problem. The control for the augmented problem is the rate of change, \tilde{v}_{xk} . For the augmented problem, we will consider a feedback control of the form

$$\tilde{v}_{xk} = -K_x \tilde{y}_{xk} - K_u \tilde{u}_{xk} - K_I \tilde{I}_k \quad (21)$$

The augmented system for the feedback problem can be obtained by augmenting the state, measurement and control vectors as well as the plant and measurement noise vectors as shown below.

$$\tilde{X}_k = \begin{pmatrix} \tilde{x}_k \\ \tilde{u}_{xk} \\ \tilde{I}_k \end{pmatrix} \quad \tilde{Y}_k = \begin{pmatrix} \tilde{y}_{xk} \\ \tilde{u}_{xk} \\ \tilde{I}_k \end{pmatrix} \quad (22)$$

$$\tilde{v}_k = \tilde{v}_{xk} \quad (23)$$

$$w_k = \begin{pmatrix} w_{xk} \\ w_{uk} \\ w_{lk} \end{pmatrix} \quad v_k = \begin{pmatrix} v_{xk} \\ v_{uk} \\ v_{lk} \end{pmatrix} \quad (24)$$

Combining the state and measurement perturbation equations in (17) and (18) with the control rate and integrator equations in (19) and (20), and using the augmented state and measurement vectors in (22) - (24) along with control equation in (21), it is possible to express the augmented feedback control problem in the following form.

$$\tilde{X}_{k+1} = \Phi \tilde{X}_k + \Gamma \tilde{v}_k + w_k \quad (25)$$

$$\tilde{Y}_k = C \tilde{X}_k + \tilde{v}_k \quad (26)$$

where the augmented system matrices are defined appropriately in terms of the original perturbation system matrices. The feedback control is restricted to the form

$$\tilde{v}_k = -K \tilde{Y}_k = - \begin{pmatrix} K_x & K_u & K_l \end{pmatrix} \begin{pmatrix} \tilde{y}_{xk} \\ \tilde{u}_{xk} \\ \tilde{l}_k \end{pmatrix} \quad (27)$$

Thus, the augmented problem also has the form of a discrete stochastic system with measurements consisting of linear combinations of the state corrupted by the augmented white noise process. Selecting a quadratic cost function, we have

$$J(K) = \lim_{N \rightarrow \infty} \frac{1}{2(N+1)} E \left\{ \sum_{k=0}^N \tilde{X}_{k+1}^T Q \tilde{X}_{k+1} + \tilde{v}_k^T R \tilde{v}_k \right\} \quad (28)$$

The feedback control problem can now be posed as follows. Find a feedback control \tilde{v}_k which minimizes the selected quadratic cost function (28) subject to the constraints given by (25) -(27). This is precisely the discrete Stochastic Optimal Feedback problem discussed in [3] and can be solved using the algorithm developed therein. The variable-gain version of the problem is discussed and solved in [5]. Also note that cross-terms can be included in the cost function by introducing a preliminary feedback (see [10], p242).

2. The SOFFT Control Structure

The problem formulation described in the previous section is used to design two optimal control laws: 1) a feedforward control law whose objective is to track the pilot's input commands and produce specified flying qualities or, more generally, to produce a specified response in certain variables, and 2) a feedback control law whose objective is to maintain the deviations of the actual trajectory from the commanded one as small as possible despite noises, disturbances, nonlinearities, etc. by feeding back measurements of the actual variables. The formulation of the problem also produces a specific system structure which integrates the feedforward and the feedback control laws so that they cooperate with each other. Figures 2 and 3 show this organization of the overall control law to which we shall refer as the SOFFT Control Structure.

The control command sent to the plant is the sum of two components: one generated by the feedforward controller and the other generated by the feedback controller as shown in

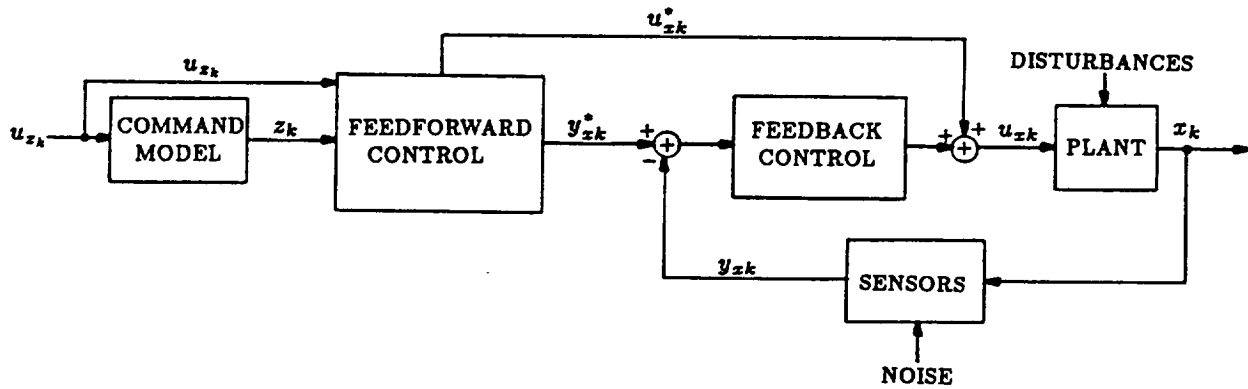


Figure 2. SOFFT Control Structure

equation (3). The feedforward control system is obtained by implementing equations (4), (5), (6) and (10) which compute the two output vectors of the feedforward control law, namely u_{xk}^* and y_{xk}^* . The only input of the feedforward control law is the pilot input command vector u_{xk} . On the other hand, the feedback control law is obtained by implementing equations (21), (19) and (20) with no noise terms. The output of the

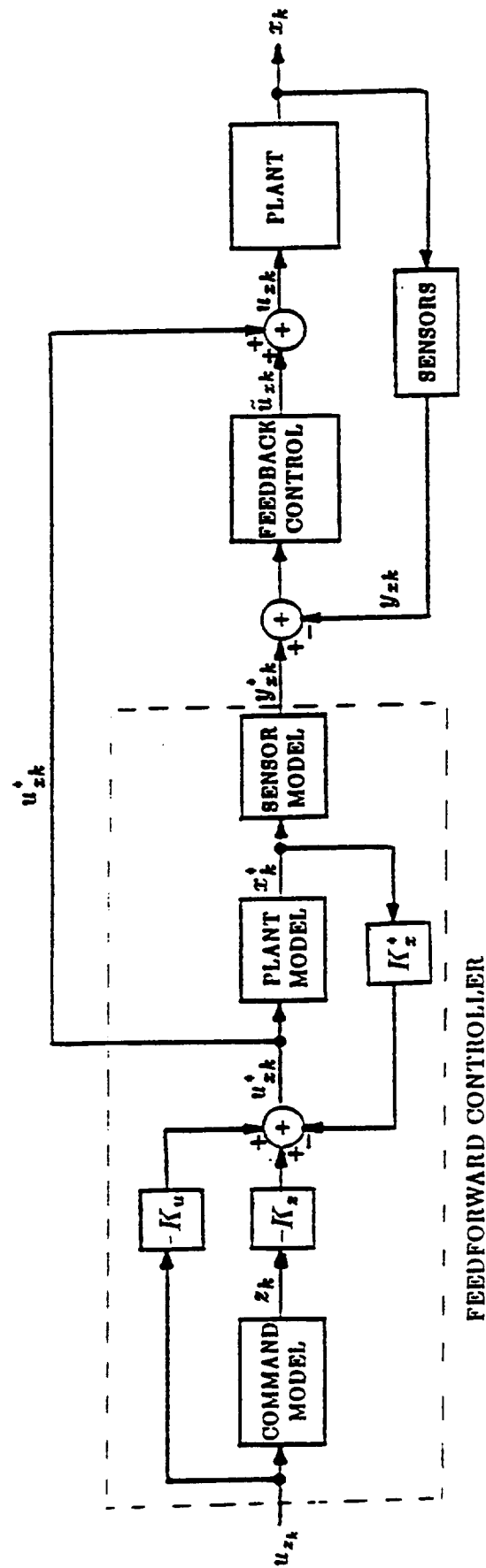


Figure 3. SOFFT Control Law Structure

feedback control system is \tilde{u}_{xx} which adds to the feedforward control u_{xx}^* to produce the total input to the plant.

Considering only the structure of the SOFFT control law, as opposed to the formulation or methodology, we note two important characteristics which distinguish it from other control laws such as the explicit model follower, the Command Generator Tracker (CGT), error feedback controller, etc.

- 1) The feedforward control law contains dynamic compensation beyond the command model, and
- 2) The feedforward control enters the feedback loop at two separate points with u_{xx}^* and y_{xx}^* .

It is also important to note that these two feedforward links (i.e., u_{xx}^* and y_{xx}^*) are highly correlated to each other. As can be seen from Figure 3, the correlation between these two vectors is introduced by the plant and sensor models used in the feedforward control law. When these models perfectly match the actual plant and sensor dynamics and no noises or disturbances are present, the actual sensor output vector, y_{xx} , equals the feedforward measurement vector, y_{xx}^* , at every sampling instant. Accordingly, no feedback correction is needed. When the models used in the feedforward control law do not match the actual plant and sensor dynamics, or random noises and disturbances are present, then the actual sensor output, y_{xx} , will deviate from the feedforward measurement or sensor vector, y_{xx}^* . Accordingly, the feedback control system will produce a corrective control action through \tilde{u}_{xx} . Thus, the feedforward and feedback control systems cooperate with each other and try to achieve all the control objectives.

Finally, we should point out that the block diagrams shown here should be interpreted in a functional sense, not as the implementation diagrams. For implementation, we recommend using an incremental implementation (see [1], [2]) of the control laws. **A new incremental implementation which is intended for systems having both control position and control rate limiters is given in Appendix A.**

B. INTEGRATED SOFFT CONTROL: A NEW APPROACH

It is well-known that, for a continuous linear system with Gaussian statistics and a quadratic cost function, the optimal, causal or non-anticipative feedback control law is one that feeds back the least-mean-square estimate of the state vector [11]. It is also well-known that this result remains valid for sampled-data systems with Gaussian statistics [10]. It follows that, when a system consists of two or more linear subsystems which have Gaussian statistics, quadratic cost functions and are also "uncoupled", the optimal control for the overall system will consist of uncoupled optimal control laws for each of the subsystems, provided that "uncoupled" is properly defined.

In this context, we consider the subsystems "uncoupled" if

- 1) their dynamical models are not coupled,
- 2) the plant and measurement noises and the initial state for each subsystem are uncorrelated to the plant and measurement noises and the initial state of the other subsystems,
- 3) the measurement vector is uncoupled; i.e., each measurement is a linear combination of the state of only one subsystem, corrupted by white measurement noise, and
- 4) the cost function for the overall system can be written as the sum of quadratic cost functions for each subsystem.

Under the conditions stated above, each subsystem will be independent of the others. It is easy to see that the optimal control for each subsystem will produce the optimal control for the overall system which will consist of a set of uncoupled sub-control laws.

The conclusion we draw from this observation is that **if the subsystems are uncoupled, we cannot improve the closed-loop performance by introducing coupling through the feedback control law.** The cross-coupling of the subsystems introduced through an "integrated" control law will not improve the system's performance.

Now consider the feedforward control law within the context of the SOFFT control formulation described in the previous sections. In the feedforward control case, it seems clear that the command model itself which is selected by the control designer needs to be uncoupled. For example, if we want to command the sum of two variables which come from different subsystems, it is clear that the optimal feedforward control law would have to be coupled at least for the two subsystems involved. However, if the command model consists of uncoupled command models for each subsystem, then the SOFFT feedforward control law for perfect tracking would also be uncoupled, provided that the necessary matrix inverse exists. **Thus, in the case of the feedforward control, we must further consider whether the command model is coupled.**

On the other hand, let us consider a system with some degree of cross-coupling among its subsystems. The optimal feedback control law for this system will, in fact, contain some degree of cross-coupling. In other words, in comparison to uncoupled control systems, **an "integrated" control law can improve the performance of a coupled open-loop system** . But we would expect that the amount of improvement obtained by the use of a coupled control law would depend on the degree of coupling present in the open-loop system. In other words, for a loosely coupled open-loop system, the performance degradation resulting from the use of an uncoupled control law would be smaller than that which would result for a highly coupled open-loop system.

Similar observations can be made about the feedforward control law. When the system has some degree of coupling among its subsystems, the optimal feedforward control law will also contain cross-coupling terms among the subsystems. Also, we would expect that the amount of coupling in the feedforward control law would be, in some sense, proportional to the degree of coupling present in the open-loop system.

To understand the advantages and disadvantages of designing an integrated control law more clearly, we will start by developing the mathematical formulation of the integrated control problem.

1. Problem Formulation

Suppose that we have already discretized the continuous open-loop system under consideration at the desired sampling rate, Δt . Thus, we have a discrete linear system of the form shown in (1) and (2) which we will repeat here for ease of reference.

$$x_{k+1} = \Phi_x x_k + \Gamma_x u_{xk} + w_{xk} \quad (1)$$

$$y_{xk} = C_x x_k + v_{xk} \quad (2)$$

We consider these equations to represent the overall or integrated open-loop system model which consists of several subsystems. Suppose that we have L subsystems which have varying degrees of coupling with each other. We will consider the first subsystem to be the main system which we want to control unless specified otherwise. For example, in our aircraft example, the first subsystem would be the airframe dynamics subsystem and the second subsystem would be the propulsion dynamics subsystem. However, this is a completely arbitrary selection and has no influence on the development of the integrated control law.

Let the i^{th} subsystem state vector at the k^{th} sampling instant be denoted by x_{ik} . Let the i^{th} state vector, x_{ik} , have the dimension n_{x_i} . Similarly, let the i^{th} subsystem measurement vector, y_{xik} , have the dimension n_{y_i} . The i^{th} subsystem model can be expressed in the form

$$x_{ik+1} = \Phi_{xii} x_{ik} + \Gamma_{xii} u_{xik} + \sum_{\substack{j=1 \\ j \neq i}}^L \{ \Phi_{xij} x_{jk} + \Gamma_{xij} u_{xjk} \} + w_{xik}, \quad i = 1, 2, \dots, L \quad (29)$$

$$y_{xik} = C_{xii} x_{ik} + \sum_{\substack{j=1 \\ j \neq i}}^L C_{xij} x_{jk} + v_{xik}, \quad i = 1, 2, \dots, L \quad (30)$$

The terms included in the summation sign describe the cross-coupling terms between the i^{th} subsystem and the remaining subsystems. According to the degree of coupling that exists, these terms can be null, small or large.

The integrated state and measurement vectors can be obtained by augmenting the subsystem state and measurement vectors as shown below.

$$x_k = \begin{pmatrix} x_{1k} \\ x_{2k} \\ \vdots \\ x_{Lk} \end{pmatrix} \quad y_{xk} = \begin{pmatrix} y_{x1k} \\ y_{x2k} \\ \vdots \\ y_{xLk} \end{pmatrix} \quad (31)$$

The integrated control vector, as well as the plant and measurement noise vectors, can be obtained in the same manner.

$$u_{xk} = \begin{pmatrix} u_{x1k} \\ u_{x2k} \\ \vdots \\ u_{xLk} \end{pmatrix} \quad w_{xk} = \begin{pmatrix} w_{x1k} \\ w_{x2k} \\ \vdots \\ w_{xLk} \end{pmatrix} \quad v_{xk} = \begin{pmatrix} v_{x1k} \\ v_{x2k} \\ \vdots \\ v_{xLk} \end{pmatrix} \quad (32)$$

The integrated open-loop system matrices in (1) and (2) can be expressed in terms of the subsystem matrices in (29) and (30) as follows.

$$\Phi_x = \begin{pmatrix} \Phi_{x11} & \Phi_{x12} & \cdots & \Phi_{x1L} \\ \Phi_{x21} & \Phi_{x22} & \cdots & \\ \vdots & \vdots & \ddots & \vdots \\ \Phi_{xL1} & & \cdots & \Phi_{xLL} \end{pmatrix} \quad (33)$$

$$\Gamma_x = \begin{pmatrix} \Gamma_{x11} & \Gamma_{x12} & \cdots & \Gamma_{x1L} \\ \Gamma_{x21} & \Gamma_{x22} & \cdots & \\ \vdots & \vdots & \ddots & \vdots \\ \Gamma_{xL1} & & \cdots & \Gamma_{xLL} \end{pmatrix} \quad (34)$$

$$C_x = \begin{pmatrix} C_{x11} & C_{x12} & \cdots & C_{x1L} \\ C_{x21} & C_{x22} & \cdots & \\ \vdots & \vdots & \ddots & \vdots \\ C_{xL1} & & \cdots & C_{xLL} \end{pmatrix} \quad (35)$$

2. A SOFFT Approach to Integrated Control

The basic approach we recommend is to use a feedback control law with limited coupling, obtained by constrained optimization, driven by a centralized perfect tracking feedforward control law. In the following, we will describe why we view this as best approach. With that in mind, we first discuss why an uncoupled control law needs higher performance margins, then we consider the advantages and disadvantages of using a fully centralized control law, particularly for the feedback loops, and finally, we discuss why the best solutions for the feedback and feedforward control laws may be quite different.

As described in the introduction of Section II, in comparison to an uncoupled control law, an integrated control law can improve the performance of a coupled open-loop system. In this context, improved performance is not simply more accurate tracking of input commands although that is certainly one of the important performance criteria. We mean that both the feedforward objectives (command tracking, transient response, etc) and the feedback objectives (stability, noise attenuation, disturbance accommodation, etc.) can be improved by the appropriate use of an integrated control law.

In this work, by an integrated control law, we mean one which contains some coupling between some of the subsystems, but not necessarily all of the subsystems. In other words, while a centralized full-state feedback (or output feedback) control law is an integrated control law and an uncoupled control law is not, most integrated control laws will be in between these two extremes and contain only a limited amount of coupling between a limited number of subsystems.

Coupling as Disturbance

In the preceding paragraphs, we have discussed the advantages and disadvantages of using a fully centralized control law (e.g., a full state feedback control law with or without a Kalman filter) as the integrated control. Now consider the implications of an uncoupled control law.

The usual approach used in many designs is to ignore the coupling among subsystems and obtain control laws for each subsystem. This, of course, results in an uncoupled control law. **The implication of this approach is to interpret the coupling among the various subsystems as disturbances.**

This can be seen more clearly by considering equations (29) and (30) of the problem formulation. When designing separate control laws for each subsystem, the designer automatically considers the coupling terms in the summation sign as an independent disturbance rather than a coupled signal with its own modes. More often, the designer does not even include these terms in the design model, but simply assumes that it is not present. In other words, the terms in brackets below are either eliminated or viewed as a disturbance.

$$x_{ik+1} = \Phi_{xi} x_{ik} + \Gamma_{xi} u_{xi k} + \left[\sum_{\substack{j=1 \\ j \neq i}}^L \{ \Phi_{xj} x_{jk} + \Gamma_{xj} u_{xj k} \} + w_{xi k} \right] \quad (29)$$

$$y_{xi k} = C_{xi} x_{ik} + \left[\sum_{\substack{j=1 \\ j \neq i}}^L C_{xj} x_{jk} + v_{xi k} \right] \quad (30)$$

If the coupling terms are not in the design model and, therefore, are not used in the control law directly, but are present in the real system, their impact will be to degrade the performance of the closed-loop system. Therefore, the designer must increase the performance margins for the uncoupled design beyond the usual level. By performance margin, we mean a margin for each design objective for both the feedback and the feedforward control laws. For example, the feedback system must have a higher stability margin, say a phase and gain margin in each feedback loop. Therefore, one of the most

important implications of using an uncoupled control law is that **the performance margins must be increased to accommodate the coupling terms as pseudo-disturbances**. Even then, the actual performance (e.g., command tracking error, noise attenuation, etc.) cannot reach the level possible with an integrated control law.

Centralized or Integrated

Since a fully centralized control law (e.g., a full state feedback control law with or without a Kalman filter) can improve the performance of the integrated open-loop system, at first, this may seem like the best approach to integrated control design. However, for practical systems of some complexity which usually also contain various types of nonlinearities, there are some disadvantages to the use of centralized control laws.

One of the disadvantages of a fully centralized control law is its complexity of the control law itself and the complexity of the closed-loop system. For high order systems with multiple high order subsystems, even the implementation of the control law and testing/validation of the control software on the flight computer can be a difficult task.

More importantly, a fully centralized control law feeds every subsystem variable to every subsystem control. In other words, even subsystems which are only coupled to a negligible degree, will be coupled further through the control law. This type of coupling of essentially uncoupled systems, or of essentially independent variables, is likely to produce complexity without a corresponding significant benefit in performance. However, by coupling essentially independent modes of otherwise independent subsystems, we may be introducing unnecessary dependencies between subsystems. For example, undesired nonlinear behaviour or high noises in one subsystem could enter all the other subsystems.

Furthermore, most physical systems of practical importance contain significant nonlinearities which include varying parameter values, limiters, rate limits, saturation, etc. When implementing such real-life systems, it is vital for the designer to fully understand all the implications of the control law's behaviour under many scenarios, particularly under scenarios in which the nonlinear regions of the subsystems have been entered. When one considers that **each subsystem may have completely different regions of nonlinear behaviour**, the bounds of simple linear analysis are reached quickly. When one also includes safety considerations under common subsystem failures, it becomes clear that

simplicity is an often misunderstood but very important virtue in control system design. Introducing complexity without a significant benefit should be avoided

Finally, subsystem validation is an important part of the procedure before a flight test to ascertain the integrity of all the subsystems under the various circumstances of flight. If the closed-loop subsystem is coupled to all the other subsystems, it may lose its intrinsic characteristics. For example, the subsystem inputs may now come from some usually unrelated subsystem. **The validation and testing of the subsystem becomes more complicated.** An established testing procedure may not always be available for highly complex situations. Thus, the benefits of the added complexity must be sufficient to outweigh the disadvantages introduced in the process.

Considering the various advantages and disadvantages of integrating the control law, it seems clear that a compromise in which some, but not all, the subsystems and variables are coupled is the best approach. In particular, **for feedback control, the guiding principle may be to avoid coupling the subsystems except where a distinct improvement can be obtained.**

We consider the implications of the discussion above for the feedforward and the feedback control laws in the following section.

Different Strokes...

In this section, we discuss the type of integration that is most suitable for the feedback and the feedforward control laws within the SOFFT context. We think that the feedback control law should contain limited cross-coupling among the subsystems, while the feedforward control law is best centralized. **Because the feedforward and feedback control laws have completely different objectives, we arrive at different solutions for the two control laws.** Thus, we have different solutions for different objectives.

We will first consider the feedback control law. Recall that the major objectives of the SOFFT feedback control law are to provide stability, noise attenuation, disturbance accommodation and robustness of these characteristics while the feedforward control law is trying to track the input commands. All the disadvantages discussed in the previous

section apply to the feedback control law: complexity of implementation, subsystem validation difficulties, understanding behaviour in nonlinear regions, etc.

Because of all these reasons, we think that the best approach to the feedback control design is to introduce coupling only among variables which are already coupled. If the variables and the subsystems are already coupled, the extra coupling produced by the control law does not really add new complexity since the designer will have to understand the coupling between the subsystems anyway. On the other hand, since the variables and subsystems are coupled, the control law is likely to achieve better performance when it is not restricted.

Since the open-loop system model for the integrated system ((29), (30)) has been augmented into the same form as the single or centralized system equations ((1),(2)), the integrated feedback control formulation follows precisely the same procedure until we are ready to introduce the coupling constraints.

For the PIF (Proportional-Integral-Filter) control structure that we are considering, the feedback control law has the form

$$\tilde{v}_k = -K \tilde{Y}_k = - \begin{pmatrix} K_x & K_u & K_I \end{pmatrix} \begin{pmatrix} \tilde{y}_{xx} \\ \tilde{u}_{xx} \\ \tilde{I}_k \end{pmatrix} \quad (27)$$

However, now each vector and matrix is an augmented version of the original case. To constrain coupling between any two subsystems through the control law, we simply must constrain the corresponding elements of the augmented gain matrix, K , to vanish. Thus, no communication link will be present between the corresponding variables of the subsystems involved.

While setting the desired elements of the gain matrix to zero formulates the problem to be solved, note that the Stochastic Output Feedback algorithm [3] does not provide for this type of constraint in the optimization algorithm. Therefore, we must develop an output feedback algorithm which can optimize the feedback gain matrix subject to the constraints set above. This problem will be addressed in greater detail in Section III both for time

invariant or single model problems, as well as for the multi-model case with a variable-gain matrix for potential application to nonlinear problems [5], [1].

Now, consider the feedforward control integration problem. In the SOFFT methodology, the main feedforward control objective is to produce the desired system response to the input commands by tracking the command model outputs with no noise or disturbance present. It is important to note that **the feedforward control law does not have any effect on the closed-loop system stability**. This can be easily verified by observing, say in Figure 2 or 3, that the feedforward control law is in series with the closed-loop plant. Thus, as long as the feedforward control law itself is stable, it does not change the stability characteristics of the closed-loop plant even as the plant parameters vary or other nonlinearities occur.

Therefore, for purposes of understanding the stability of the system, the complexity of the feedback control law makes the analysis of stability and its various robustness criteria more complex; however, the feedforward control law does enter this difficult part of the analysis.

Similarly, by the definition of the feedforward control problem in the SOFFT context, the feedforward control law leaves the objective of noise attenuation to the feedback control law. The feedforward control law uses only pilot input commands, but has no access to the measurements obtained by the sensors. Accordingly, it cannot attenuate the random noises which enter the system. Thus, the feedforward control does not contain any noise in its variables except for computer round-off errors which are occurring in the flight computer on board. In most of the computers used today, these noise levels are negligible. Therefore, introducing unnecessary noises from one subsystem to another is not a consideration in the feedforward control law.

It should be noted that the validation of plant subsystems can be performed irrespective of the type of feedforward used. As long as the feedback control is designed in a manner that maintains the identity of a subsystem, the feedforward subsystem inputs coming from u_{xx}^* and y_{xx}^* to that subsystem only can be used in the validation.

The accommodation of random or known disturbances is left to the feedback control law which has access to the measurements and can feed them back to ensure that the system is,

in fact, where it ought to be. The feedforward control law does not attempt to accommodate disturbances. As discussed in a previous section, ignoring the coupling among subsystems corresponds to treating them as unknown disturbances. If the coupling among the subsystems is neglected in the design plant model, the feedforward control law will generate the wrong feedforward control and measurement vector sequences, u_{xx}^* and y_{xx}^* , respectively, which is its main objective. In other words, the desired response to input commands will not be generated correctly. It will then be necessary for the feedback control to try to correct the tracking error due to the coupling of the subsystems in a reactive manner.

Since generating the desired system response to input commands is the main objective of the feedforward control law, it seems that a significant benefit will be lost if the coupling is omitted. Therefore, **we recommend using the centralized perfect tracking feedforward control law**. Because the computation of the perfect tracking feedforward matrices is so straight-forward, it is hard to see many cases where this would produce any of the disadvantages present for the feedback control law. However, in cases where ignoring the subsystem coupling produces a benefit in the feedforward control, this can be easily accommodated using the SOFFT feedforward for each subsystem, thus obtaining an uncoupled feedforward control law.

The formulation of the integrated feedforward control law is the same as the one described Section II.A.1.

C. INTEGRATED FEEDFORWARD CONSIDERATIONS

While we have developed a promising approach to integrated control using the SOFFT philosophy for feedforward and feedback, some questions about the form of the open-loop system still remain. The first question is related to the measurements. While many sensor outputs can be described as linear combinations of the state, others require the use of the control as well as the state. We would like to include such control-dependent measurements in the formulation of the integrated SOFFT control problem.

The other question that deserves some attention is the stability of the feedforward control law when the open-loop system is unstable; i.e., the question of static instability for the

feedforward control. The feedback control stability has been studied extensively. The feedforward stability for unstable open-loop plants will be investigated for the integrated control problem.

1. Control-Dependent Measurements

Consider a sampled-data system; i.e., a continuous time system which will be controlled by a digital control system. Suppose that the system has control-dependent measurements of the form

$$y_x(t) = C_x x(t) + D_x u_x(t) \quad (36)$$

where t denotes time and the measurement noise term has been neglected so as to concentrate on the problem at hand.

While most measurements can be expressed without the use the control vector, some sensors measure a linear combination of the state and control vectors. These are usually sensors which measure an acceleration, a velocity or a force or moment. For example, the output of an accelerometer is a control-dependent measurement. In the example used in Section IV, we will use an accelerometer along the forward stability axis which requires the control vector. Accordingly, we will need to find a way of accommodating control-dependent measurements. One approach is given in the following.

The standard sampled-data formulation [10] assumes that the control remains constant over the sampling period, Δt .

$$u_x(t) = u_{xk}, \quad t_k = k \Delta t \leq t < (k+1) \Delta t = t_{k+1}, \quad k = 0, 1, 2, \dots \quad (37)$$

Let t'_k denote the time at which the k^{th} measurement is sampled. Thus, the measurement, $y_x(t'_k)$, is obtained at time t'_k . At this time, we can start to compute the feedback vector which is usually obtained by multiplying the measurement vector by the feedback gain matrix. Once the flight computer computes the complete control vector, the control values can be sent to the control actuator at time

$$t_k = t'_k + \Delta c = k \Delta t \quad (38)$$

where Δc denotes the amount of time required by the flight computer to compute the control vector, usually in the order of a few milliseconds. Until the new control is sent to the actuators, the sampled-data commands the previous control vector, u_{xk-1} .

From (38), it is clear that $t'_k < k \Delta t$. Thus, when the k^{th} measurement is obtained, the control vector is u_{xk-1} ; i.e., the control corresponds to the previous sampling instant. In mathematical form,

$$y_{xk} = y_x(t'_k) = C_x x(t'_k) + D_x u_x(t'_k) = C_x x_k + D_x u_{xk-1} \quad (39)$$

Therefore, for sampled-data systems, control-dependent measurements of the form shown in (36), take the following form when they are discretized.

$$y_{xk} = C_x x_k + D_x u_{xk-1} \quad (40)$$

If the original measurement was corrupted by noise, the discrete measurement will also be corrupted by a corresponding discrete noise process.

Now, we will embed a sampled-data system with control-dependent measurements into one without a dependence on the control vector. We achieve this by augmenting the state vector by the previous value of the control vector as follows. Define the vector

$$r_k = u_{xk-1} \quad (41)$$

Now, augment the state equations in the plant (1) by (41) using the augmented state vector shown below.

$$\begin{pmatrix} x_{k+1} \\ r_{k+1} \end{pmatrix} = \begin{pmatrix} \Phi_x & 0 \\ 0 & 0 \end{pmatrix} \begin{pmatrix} x_k \\ r_k \end{pmatrix} + \begin{pmatrix} \Gamma_x \\ I \end{pmatrix} u_{xk} + \begin{pmatrix} w_{xk} \\ 0 \end{pmatrix} \quad (42)$$

Now, if we express the control-dependent measurements in (40) in terms of the augmented state in the system of (42), we obtain

$$y_{\star} = \begin{pmatrix} C_x & D_x \end{pmatrix} \begin{pmatrix} x_k \\ r_k \end{pmatrix} + v_{\star} \quad (43)$$

where we have included the measurement noise in the formulation.

In (42) and (43), we have expressed the system with control-dependent measurements in the form of one which the measurements depend only on the state. Thus, the control-dependent measurement problem has been embedded in one of the form of (1) and (2). Therefore, all the results we have developed in Section II apply equally to the case of control-dependent measurements.

2. Unstable Open-loop Plant

As engineers have explored advanced aircraft new aerodynamic profiles, experimented with new aerodynamic control surfaces, tried forward-swept wing concepts and eliminated the tail section of the aircraft, the static stability of the aircraft has become a variable which depends on the particular aerodynamic design of the aircraft. Several advanced aircraft are unstable, at least in certain flight conditions. In particular, the modified F-15 SMTD aircraft which is used as an example in Section IV is open-loop unstable at the flight condition corresponding to 30° angle-of-attack.

In this section, we briefly investigate conditions under which the SOFFT feedforward control law stabilizes an open-loop unstable plant model shown in Figure 3. We will consider the "optimal tracking" and "perfect tracking" cases in that order.

Referring to the feedforward cost function given by (9) in Section II.A.1, recall that when the matrices Q_1^*, R_1^* vanish, the tracking error can also vanish resulting in the perfect tracking case. If these matrices do not vanish, then the tracking error can only be optimized to obtain the smallest level of error attainable for that cost function.

Lemma 1. *For the optimal feedforward control problem defined in Section II.A.1, if the open-loop system is stabilizable and detectable, then the SOFFT feedforward control gain K_x^* stabilizes the open-loop system if the cost matrices Q_1^*, R_1^* are both positive definite.*

The proof of the lemma follows directly from Theorems 6.30. and 6.31. in [12], p. 497.

It is clear that for a large class of open-loop systems, the optimal tracking feedforward control will stabilize the system even if it has static instabilities. The case of the perfect tracking feedforward control is more complicated. However, the following result applies. Define the closed-loop system matrix as shown below.

$$\overline{\Phi}_x = \Phi_x - \Gamma_x [H_x \Gamma_x]^{-1} H_x \Phi_x \quad (44)$$

Lemma 2. *For the optimal feedforward control problem defined in Section II.A.1, where the cost matrices Q_1^*, R_1^* are both null, the optimal control will stabilize the open-loop system if the system $(H_x, \overline{\Phi}_x, \Gamma_x)$ is output stabilizable and $[H_x \Gamma_x]$ is invertible.*

Proof: The proof follows directly from Theorem 1 in [3], p. 9, by noticing that the impulse response goes to zero, since

$$H_x \overline{\Phi}_x^k \Gamma_x = H_x (\Phi_x - \Gamma_x [H_x \Gamma_x]^{-1} H_x \Phi_x) \overline{\Phi}_x^{k-1} \Gamma_x = 0, \quad k \geq 1 \quad (45)$$

Thus, the impulse response matrix for this system converges to 0 as k gets large since it is null. Therefore, the closed loop system matrix for the perfect tracking case $\overline{\Phi}_x$ is stable.

The class of open-loop systems covered by these conditions is less clear. From our experience, it is quite a large class. However, we are not sure that it covers all systems of practical importance. It should be noted that, whenever necessary, one may add very small cost matrices Q_1^*, R_1^* to include the class defined by Lemma 1.

III. INTEGRATED/CONSTRAINED OUTPUT FEEDBACK CONTROL

In this section, we will formulate and develop an algorithm for the integrated or constrained stochastic output feedback control problem. The formulation will be within the SOFFT context; i.e., we formulate a problem with a feedback control law that will cooperate with a SOFFT feedforward control law. However, the algorithm developed for the feedback control gain optimization is applicable to any discrete output feedback problem.

We will first consider the single model or time-invariant problem. Then we will extend the formulation and the algorithm to the variable-gain output feedback control case to accommodate nonlinear problems with wide variations in the operating range.

A. TIME-INVARIANT PROBLEM FORMULATION

The problem formulation of the integrated output feedback control problem was started in Section II.B.1 in the process of developing a SOFFT approach to the integration of the control law. Here, we will formulate the complete problem to find the optimal solution to the problem and obtain an algorithm to compute the gain matrices which define the optimal control law.

Consider a system composed of L subsystems some of which may be coupled in their dynamics and their measurements. Note that while some measurements may contain state variables from more than one subsystem, the control variables and state variables can belong only to one subsystem. This does not apply to the measurements which may be considered part of more than one subsystem. However, care must be used in such cases

since the number of measurements increases and the measurement matrix loses its full rank property.

Now, let the i^{th} subsystem state vector at the k^{th} sampling instant be denoted by x_{ik} . Let the i^{th} state vector, x_{ik} , have the dimension n_{x_i} . Similarly, let the i^{th} subsystem measurement vector, y_{ik} , have the dimension n_{y_i} . The i^{th} subsystem model can be expressed in the form

$$x_{ik+1} = \Phi_{xi} x_{ik} + \Gamma_{xi} u_{ik} + \sum_{\substack{j=1 \\ j \neq i}}^L \{ \Phi_{xij} x_{jk} + \Gamma_{xij} u_{jk} \} + w_{ik}, \quad i = 1, 2, \dots, L \quad (29)$$

$$y_{ik} = C_{xi} x_{ik} + \sum_{\substack{j=1 \\ j \neq i}}^L C_{xij} x_{jk} + v_{ik}, \quad i = 1, 2, \dots, L \quad (30)$$

where the plant and measurement noise sequences are assumed to be zero mean white noise processes uncorrelated to each other and to the initial condition vectors.

The coupled set of subsystems can be integrated into a large single system of the usual form we have been considering in the previous sections; i.e.,

$$x_{k+1} = \Phi_x x_k + \Gamma_x u_{\star k} + w_{\star k} \quad (1)$$

$$y_{\star k} = C_x x_k + v_{\star k} \quad (2)$$

For completeness, note that the integrated state and measurement vectors can be obtained by augmenting the subsystem state and measurement vectors as shown below.

$$x_k = \begin{pmatrix} x_{1k} \\ x_{2k} \\ \vdots \\ x_{Lk} \end{pmatrix} \quad y_{\star k} = \begin{pmatrix} y_{x1k} \\ y_{x2k} \\ \vdots \\ y_{xLk} \end{pmatrix} \quad (31)$$

The integrated control vector, as well as the plant and measurement noise vectors, can be obtained in the same manner.

$$u_{xk} = \begin{pmatrix} u_{x1k} \\ u_{x2k} \\ \vdots \\ u_{xLk} \end{pmatrix} \quad w_{xk} = \begin{pmatrix} w_{x1k} \\ w_{x2k} \\ \vdots \\ w_{xLk} \end{pmatrix} \quad v_{xk} = \begin{pmatrix} v_{x1k} \\ v_{x2k} \\ \vdots \\ v_{xLk} \end{pmatrix} \quad (32)$$

The integrated open-loop system matrices in (1) and (2) can be expressed in terms of the subsystem matrices in (29) and (30) as follows.

$$\Phi_x = \begin{pmatrix} \Phi_{x11} & \Phi_{x12} & \cdots & \Phi_{x1L} \\ \Phi_{x21} & \Phi_{x22} & \cdots & \\ \vdots & \vdots & \ddots & \vdots \\ \Phi_{xL1} & & \cdots & \Phi_{xLL} \end{pmatrix} \quad (33)$$

$$\Gamma_x = \begin{pmatrix} \Gamma_{x11} & \Gamma_{x12} & \cdots & \Gamma_{x1L} \\ \Gamma_{x21} & \Gamma_{x22} & \cdots & \\ \vdots & \vdots & \ddots & \vdots \\ \Gamma_{xL1} & & \cdots & \Gamma_{xLL} \end{pmatrix} \quad (34)$$

$$C_x = \begin{pmatrix} C_{x11} & C_{x12} & \cdots & C_{x1L} \\ C_{x21} & C_{x22} & \cdots & \\ \vdots & \vdots & \ddots & \vdots \\ C_{xL1} & & \cdots & C_{xLL} \end{pmatrix} \quad (35)$$

Thus, the integrated system can be expressed as a standard discrete linear system as given in (1) and (2) as shown above. Accordingly, the SOFFT developments described in Section II.A.1 for both feedforward and feedback control apply to the integrated system. Without repeating all of the equations in this section, we will consider a feedback control law with the PIF structure as described in equations (15) - (21).

The state, measurement and control vectors of the integrated system shown above can now be augmented to include the control and integrator vectors of the PIF structure as follows.

$$\tilde{X}_k = \begin{pmatrix} \tilde{x}_k \\ \tilde{u}_{xk} \\ \tilde{I}_k \end{pmatrix} = \begin{pmatrix} \tilde{x}_{1k} \\ \vdots \\ \tilde{x}_{Lk} \\ \tilde{u}_{x1k} \\ \vdots \\ \tilde{I}_{1k} \\ \vdots \end{pmatrix} \quad (46)$$

$$\tilde{Y}_k = \begin{pmatrix} \tilde{y}_{xk} \\ \tilde{u}_{xk} \\ \tilde{I}_k \end{pmatrix} = \begin{pmatrix} \tilde{y}_{x1k} \\ \vdots \\ \tilde{y}_{xLk} \\ \tilde{u}_{x1k} \\ \vdots \\ \tilde{I}_{1k} \\ \vdots \end{pmatrix} \quad (47)$$

The integrated and PIF augmented system can now be expressed as

$$\tilde{X}_{k+1} = \Phi \tilde{X}_k + \Gamma \tilde{v}_k + w_k \quad (48)$$

$$\tilde{Y}_k = C \tilde{X}_k + v_k \quad (49)$$

where the new control vector, \tilde{v}_k , is defined by (19) as the rate of change of the original control position.

For the integrated control problem we are formulating, it is necessary to constrain the control vector so that some variables are not fed back into certain subsystems. This will allow the designer to choose which subsystems and variables to couple and which not to couple within the feedback control law.

First, we constrain the control vector to use only the measurement or feedback vector including internally generated variables such as the control position vector and the integrator vector. This constrains the control to the measurement vector in (49) as the standard stochastic output feedback problem.

$$\tilde{v}_k = -K \tilde{Y}_k = - \begin{pmatrix} K_x & K_u & K_I \end{pmatrix} \begin{pmatrix} \tilde{y}_{xk} \\ \tilde{u}_{xk} \\ \tilde{I}_k \end{pmatrix} \quad (50)$$

Showing the details of the subsystem partitions results in

$$\begin{pmatrix} \tilde{v}_{x1k} \\ \tilde{v}_{x2k} \\ \vdots \\ \tilde{v}_{xLk} \end{pmatrix} = - \begin{pmatrix} K_{x11} & \cdots & K_{x1L} & K_{u11} & \cdots & K_{u1L} & K_{I11} & \cdots & K_{I1L} \\ K_{x21} & \ddots & \vdots & K_{u21} & \ddots & \vdots & K_{I21} & \ddots & \vdots \\ \vdots & & & \vdots & & & \vdots & & \\ K_{xL1} & \cdots & K_{xLL} & K_{uL1} & \cdots & K_{uLL} & K_{IL1} & \cdots & K_{ILL} \end{pmatrix} \begin{pmatrix} \tilde{y}_{x1k} \\ \vdots \\ \tilde{y}_{xLk} \\ \tilde{u}_{x1k} \\ \vdots \\ \tilde{I}_{1k} \\ \vdots \end{pmatrix} \quad (51)$$

where K_{xij} , K_{uij} and K_{Iij} have the dimensions $n_{u_i} \times n_{y_j}$, $n_{u_i} \times n_{u_j}$ and $n_{u_i} \times n_{I_j}$, respectively. Equation (51) describes the integrated control feeding back the specified feedback vector for the PIF structure. However, to avoid coupling the subsystems, or more generally, to avoid coupling a feedback variable to a control component for whatever subsystem, it is necessary to place additional constraints on the form of the control law. We can achieve this result by constraining certain elements of the feedback gain matrix to vanish; i.e., the control designer sets certain gain elements to zero.

For example, note that if we constrain the partitioned gain matrices K_x , K_u and K_I to be block diagonal, that is we constrain the off-diagonal blocks to be zero, the resulting feedback control system will be completely uncoupled. Since, the only nonzero blocks in the gain matrix are on the diagonal, each subsystem control will have the form

$$\tilde{v}_{xik} = -K_{xii} \tilde{y}_{xik} - K_{uii} \tilde{u}_{xik} - K_{Iii} \tilde{I}_{ik}, \quad i = 1, 2, \dots, L \quad (52)$$

Each control feeds back only the measurements related to its own subsystem and, therefore, the control law is uncoupled. On the other hand, if the designer wants to allow some coupling between two subsystems, he simply does not set the corresponding blocks to zero.

In fact, note that **the coupling through the feedback control law can be one-sided**. In other words, we can feed back measurements from subsystem j to subsystem i by allowing some gains in the blocks K_{xj} , K_{uj} or K_{Ij} to be nonzero; i.e., by not constraining them to be zero. However, we do not necessarily have to feedback measurements from subsystem i to subsystem j . Thus, subsystem i may be influenced by subsystem j ; however, subsystem j need not be influenced by any other subsystem.

It is important to note that we can distinguish between the particular variables within the subsystems. Thus, we may feed one or two variables into a given control component in some subsystem. This is achieved by setting all the gains except the desired ones to zero.

Finally, note that it is not sufficient to set the off-diagonal blocks in K_x (the sensor feedback gain partition) to zero if you want to avoid coupling subsystems. You must also set the off-diagonal blocks in K_u and in K_I to zero to avoid coupling the desired subsystems through cross-terms in integral feedback or control feedback.

A simple way in which we can set specified elements of a matrix to zero is by defining the following element by element multiplication of two matrices which we shall denote by " \times ". We define the $i j$ element of the matrix product as the product of the $i j$ elements of each matrix. Thus, let the matrices K and Z have the same dimension. Then, the elements of their \times -product is given by

$$[K \times Z]_{ij} = K_{ij} Z_{ij} \quad (53)$$

Now, define the matrix Z to have elements which are either zero or 1. If you want to constrain an element of the gain matrix K to zero, then set the corresponding element of the matrix Z to zero while leaving all its other elements set to 1. Then, the product $K \times Z$ will have zero's for the specified elements while the others will be unchanged.

Select the feedback cost function

$$J(K) = \lim_{N \rightarrow \infty} \frac{1}{2(N+1)} E \left\{ \sum_{k=0}^N \tilde{X}_{k+1}^T Q \tilde{X}_{k+1} + \tilde{v}_k^T R \tilde{v}_k \right\} \quad (54)$$

Then the optimal control problem for integrated/constrained output feedback can be posed as follows. Find a stabilizing control gain matrix K which minimizes the cost function in (54) subject to the constraints in (48), (49), (50) and (55).

$$K = K \times Z \quad (55)$$

The constraint in (55) requires that the allowable gain matrices must have zero's wherever Z has zero's as specified by the control system designer. Thus, we have an additional constraint beyond those in the standard output feedback problem. We will consider the optimization of this problem in the following section.

B. ALGORITHM DEVELOPMENT

With the exception of the constraint in equation (55), the problem posed in the previous section was solved in [3]. A similar problem posed for continuous time, constant gain control laws is treated in [13] using a different approach. Here, we will follow a similar approach to the one used in [3] and then extend this development to the case of the variable-gain output feedback treated in [5].

1. Necessary Conditions

Following the approach in [3], let us define the set, S , of stabilizing gain matrices as follows.

$$S = \left\{ K \mid \rho(\Phi(K)) < 1 \right\} \quad (56)$$

where ρ denotes the spectral radius of the matrix and $\Phi(K)$ is the system matrix with the loop closed by the unconstrained gain matrix, K , as shown below.

$$\Phi(K) = \Phi - \Gamma K C \quad (57)$$

For a stabilizing gain, the cost function shown in (54) is known to be finite. So if the system is output stabilizable, S is not empty. However, we now have the further constraint of (55) which zeros out certain elements of the gain matrix. Accordingly, we need to define the constrained set of stabilizing gains which we denote by S_z .

$$S_z = \{K \in S \mid K \times Z = K\} \quad (58)$$

If the set of constrained stabilizing gains, S_z , is not empty, then a finite cost exists and the optimization problem posed is well-defined.

From Lemma 10 in [3] (pp. 19 - 20), the cost function is continuously differentiable on S and the gradient of the cost function exists and is given by

$$\frac{\partial J}{\partial K}(K) = \hat{P}(K) K \hat{S}(K) - \Gamma^T P(K) \Phi S(K) C^T, \quad K \in S \quad (59 a)$$

Since S_z is a subset of S , the expression for the gradient also holds on S_z . However, this expression of the gradient shows nonzero gradient values in all locations; i.e., even if an element of K has been set to zero, the gradient would show as a nonzero value at the corresponding location. The reason is that this expression does not take into account that the gain element is fixed at zero so that the derivative of the cost with respect to it is also zero. We want to maintain the matrix form of the gradient. Thus, we are setting the corresponding elements to zero. Another formulation could leave those elements completely out of the gradient at the expense that the matrix form would be lost.

For the integrated/constrained stochastic output feedback problem, the gradient can be expressed as

$$j(K) = \left[\hat{P}(K) K \hat{S}(K) - \Gamma^T P(K) \Phi S(K) C^T \right] \times Z, \quad K \in S_z \quad (59 b)$$

where $j(K)$ denotes the constrained gradient and the matrices used in the gradient are defined by the Lyapunov equations below.

$$P(K) = \Phi(K)^T P(K) \Phi(K) + C^T K^T R K C + Q \quad (60)$$

$$S(K) = \Phi(K) S(K) \Phi(K)^T + \Gamma K V K^T \Gamma^T + W \quad (61)$$

$$\hat{P}(K) = \Gamma^T P(K) \Gamma + R \quad (62)$$

$$\hat{S}(K) = C S(K) C^T + V \quad (63)$$

Thus, using Lemma 3 below, we can obtain the necessary conditions for the Integrated/Constrained Output Feedback Problem by setting the gradient to zero.

$$\left[\hat{P}(K) K \hat{S}(K) \right] \times Z = \left[\Gamma^T P(K) \Phi S(K) C^T \right] \times Z, \quad K \in S_z \quad (64)$$

Therefore, the optimal gain, K , must satisfy the necessary conditions shown in (64) and any gain that satisfies (64) is a critical point of the optimization problem.

2. Constrained Algorithm

Whereas we know that the optimal gain must satisfy the necessary conditions, solving (64) directly is not an easy matter. Furthermore that would only give us a critical point of the cost function. To solve the optimization problem, we must find a gain that minimizes the cost function. Accordingly, we use that idea to develop the algorithm. In other words, **given a starting gain, we will try to find a new gain which reduces the cost function and keep doing that until some convergence criterion is met.** At each iteration, we shall add an increment to the gain going in a direction which reduces the cost.

Recall the **incremental cost** which was instrumental in developing the algorithm in [3]. We will use that concept in the current problem as well.

$$\Delta J(K, \Delta K) = J(K + \Delta K) - J(K) \quad (65)$$

$$= \frac{1}{2} \text{tr} \left\{ 2 \Delta K^T \left[\hat{P}(K + \Delta K) K \hat{S}(K) - \Gamma^T P(K + \Delta K) \Phi S(K) C^T \right] \right. \\ \left. + \Delta K^T \hat{P}(K + \Delta K) \Delta K \hat{S}(K) \right\}, \quad K \in S, (K + \Delta K) \in S \quad (66)$$

Rearranging the terms in (66), it can be rewritten as ([3], p.22, Eq. (80))

$$\Delta J(K, \Delta K) = \frac{1}{2} \text{tr} \left\{ 2 \Delta K^T \frac{\partial J}{\partial K}(K) + \Delta K^T \hat{P}(K) \Delta K \hat{S}(K) + O^2(\Delta K) \right\} \quad (67)$$

Before continuing with the development of the constrained algorithm, we need to establish some elementary properties of the matrix product \times defined in (53).

Lemma 3. Let A , B and Z be matrices of appropriate order. Let all the elements of Z be 1 or 0. Then,

$$A \times Z = Z \times A \quad (68)$$

$$(A + B) \times Z = A \times Z + B \times Z \quad (69)$$

$$Z \times Z = Z \quad (70)$$

$$(A \times Z)^T = A^T \times Z^T \quad (71)$$

$$\|A \times Z\| \leq \|A\| \quad (72)$$

$$\text{tr}\{(Z \times A)B\} = \text{tr}\{A(B \times Z^T)\} \quad (73)$$

Proof: The assertions in (68) - (72) are immediate implications of the definition in (53). We will only show the validity of (73) here.

$$\text{tr}\{(Z \times A)B\} = \sum_{i,k} (Z_{ik} A_{ik}) B_{ki} = \sum_{i,k} A_{ik} (B_{ki} Z_{ki}^T) = \text{tr}\{A(B \times Z^T)\} \quad (74)$$

which shows the desired result.

Suppose that we have a stabilizing gain, K , that satisfies (55). We want to find a direction, $d(K)$, in which the cost can be reduced. Now, consider the direction matrix

$$d(K) = - \left[\hat{P}(K)^{-1} j(K) \hat{S}(K)^{-1} \right] \times Z, \quad K \in S_z \quad (75)$$

Thus, we will look for a new gain along the direction $d(K)$. If K_i is the gain for the i^{th} iteration of the algorithm, we define the next gain as

$$K_{i+1} = K_i + \alpha d(K_i), \quad i = 0, 1, 2, \dots \quad (76)$$

where α is a positive number greater than zero. From (67), it is clear that if the first term in the trace is negative then the cost along the given direction will start by going down. This is due to the fact that all the other terms in the cost function are of second order in α . If α is selected to be small enough, then the first order term will dominate the incremental cost and the next gain will reduce the cost. Thus, consider only the first term in (67) to determine its sign.

$$\text{tr}\left\{ \Delta K^T \frac{\partial J}{\partial K}(K) \right\} = -\alpha \text{tr}\left\{ d(K)^T \frac{\partial J}{\partial K}(K) \right\} \quad (77)$$

$$= -\alpha \text{tr}\left\{ \left(\left[\hat{P}(K)^{-1} j(K) \hat{S}(K)^{-1} \right] \times Z \right)^T \frac{\partial J}{\partial K}(K) \right\} \quad (78)$$

Using the properties of the \times -product given in Lemma 3, and manipulating

$$\text{tr} \left\{ \Delta K^T \frac{\partial J}{\partial K}(K) \right\} = -\alpha \text{tr} \left\{ \left[\hat{P}(K)^{-1} j(K) \hat{S}(K)^{-1} \right]^T \left(\frac{\partial J}{\partial K}(K) \times Z \right) \right\} \quad (79)$$

From (59), note that the last term in (79) is the constrained gradient. Substituting and manipulating the transpose, we get

$$\text{tr} \left\{ \Delta K^T \frac{\partial J}{\partial K}(K) \right\} = -\alpha \text{tr} \left\{ \hat{P}(K)^{-1} j(K)^T \hat{S}(K)^{-1} j(K) \right\} < 0, \quad \forall \alpha > 0 \quad (80)$$

Therefore, the direction selected in (75) is, in fact, a descent direction which will reduce the cost function. Thus, selecting α small enough by trial and error will produce a new gain to be used as the next gain in the iterations of the algorithm.

We think that it is possible to prove the convergence of this algorithm following the same arguments as in [3]. However, this is beyond the scope of this investigation and will not be pursued here. Our experience with this algorithm indicates that it is numerically stable and convergent.

We will give the detailed steps of the algorithm for the more general variable-gain problem which is investigated in the next section.

C. EXTENSION TO VARIABLE-GAIN SYSTEMS

The Variable-Gain Output Feedback Control methodology [5] was developed to accommodate nonlinear systems with large variations in the operating range. This methodology allows the feedback gain matrix to vary with selected system parameters so that the control law can adapt to the changing dynamics of each operating point.

The Variable-Gain methodology was extended in [1] to allow the control system to use the SOFFT approach with both feedforward and feedback control laws. Let p represent the parameter vector which specifies the operating point of the system. Thus, the system matrices now vary with the parameter vector.

$$x_{k+1} = \Phi_x(p) x_k + \Gamma_x(p) u_{\text{xt}} + w_{\text{xt}} \quad (81)$$

$$y_{\text{xt}} = C_x(p) x_k + v_{\text{xt}} \quad (82)$$

Using the PIF feedback structure as shown in(17) - (27), and using the same partitioning for the coupled subsystems as described in Section III.A, we results in the design model

$$\tilde{X}_{k+1} = \Phi(p) \tilde{X}_k + \Gamma(p) \tilde{v}_k + w_k \quad (83)$$

$$\tilde{Y}_k = C(p) \tilde{X}_k + v_k \quad (84)$$

The difference from the time-invariant case treated earlier is that now the control law can also vary as the system moves through different operating points. Thus, we allow the control gain matrices to vary according to the parameter vector as shown below.

$$\tilde{v}_k = -K(p) \tilde{Y}_k = - \begin{pmatrix} K_x(p) & K_u(p) & K_I(p) \end{pmatrix} \begin{pmatrix} \tilde{y}_{\text{xt}} \\ \tilde{u}_{\text{xt}} \\ \tilde{I}_k \end{pmatrix} \quad (85)$$

For a variety of reasons too lengthy to discuss here, we place the constraint of a linear relationship between the control gain matrix and the parameter p .

$$K(p) = K_0 + \sum_{i=1}^q p_i K_i = \mathcal{K} G(p) \quad (86)$$

where \mathcal{K} is an augmented gain matrix defined as follows.

$$\mathcal{K} = \begin{pmatrix} K_0 & K_1 & \cdots & K_q \end{pmatrix} \quad (87)$$

$$G(p) = \begin{pmatrix} I \\ p_1 I \\ \vdots \\ p_q I \end{pmatrix} \quad (88)$$

We embed the variable-gain output feedback problem into the time-invariant or constant gain problem by redefining the measurement vector.

$$\tilde{Y}'_k = G(p)\tilde{Y}_k = G(p)C(p)\tilde{X}_k + G(p)v_k = C'(p)\tilde{X}_k + v'_k \quad (89)$$

where the new measurement equation has the same form as before although it has a higher dimension. However, with this measurement vector, the control law can now be expressed as a constant gain feedback control law. Substituting (86) and (89) into (85), note that

$$\tilde{v}_k = -K(p)\tilde{Y}_k = -\mathcal{K}G(p)\tilde{Y}_k = -\mathcal{K}\tilde{Y}'_k \quad (90)$$

Now we have a constant gain control law trying to control a system which can vary with the parameter vector, p . Selecting a representative number, say M , operating points $\{p^j, j = 1, 2, \dots, M\}$ to cover the system's operating range, we have a multi-configuration output feedback problem with the cost function

$$J'(\mathcal{K}) = \sum_{j=1}^M f_j J(K(p^j), p^j) \quad (91)$$

$$J(K(p^j), p^j) = \lim_{N \rightarrow \infty} \frac{1}{2(N+1)} E \left\{ \sum_{k=0}^N \tilde{X}_{k+1}^T Q(p^j) \tilde{X}_{k+1} + \tilde{v}_k^T R(p^j) \tilde{v}_k \right\} \quad (92 \text{ a})$$

$$J(K(p), p) = \frac{1}{2} \text{tr} \left\{ P(K(p)) W(p) \right\} + \frac{1}{2} \text{tr} \left\{ K(p)^T \hat{P}(K(p)) K(p) V(p) \right\} \quad (92 \text{ b})$$

where f_j is the weight attached to the j^{th} operating point. Now, recall that for the integrated/constrained variable-gain problem under consideration, we have the additional constraint of setting specified elements of the gain matrix to zero. It is important to note that for the variable-gain control in (86), to avoid coupling the desired subsystems, we must zero out each gain matrix, K_i , $i = 0, 1, 2, \dots, q$. Alternately, we must augment the Z matrix used for the time-invariant case. Thus, the control gains must satisfy

$$K_i \times Z = K_i, \quad i = 0, 1, \dots, q \quad (93)$$

or alternately,

$$\mathcal{K} \times Z = \mathcal{K} \quad (94)$$

$$Z = \begin{pmatrix} Z & Z & \dots & Z \end{pmatrix} \quad (95)$$

To obtain the gradient for this case, we simply use the general expression (53) in [5] and specialize it to our case.

$$j_i(\mathcal{K}) = \frac{\partial J'}{\partial K_i}(\mathcal{K}) \times Z, \quad \mathcal{K} \in S_Z \quad (96)$$

$$= \sum_{j=1}^M f_j p_i^j \left[\hat{P}_j(\mathcal{K}) K(p^j) \hat{S}(\mathcal{K}) - \Gamma_j^T P_j(\mathcal{K}) \Phi_j S_j(\mathcal{K}) C_j^T \right] \times Z, \mathcal{K} \in S_Z \quad (97)$$

$$j(\mathcal{K}) = \begin{pmatrix} j_0(\mathcal{K}) & j_1(\mathcal{K}) & \dots & j_q(\mathcal{K}) \end{pmatrix} \quad (98)$$

Integrated/Constrained Variable-Gain Feedback Algorithm

1. Embed the variable-gain problem into the MCC form by augmenting the gain matrix as described above
2. Initialize parameters: Select initial stable gain \mathcal{K}_0 , α_0 , $i = 0$, Z , etc.
3. Initialize and save matrices. For $j = 1, 2, \dots, M$

$$\Phi_j = \Phi(p^j) \quad \Gamma_j = \Gamma(p^j) \quad C_j = C(p^j) \quad C'_j = C'(p^j) = G(p^j)C_j \quad (99)$$

$$Q_j = Q(p^j) \quad R_j = R(p^j) \quad (100)$$

$$W_j = W(p^j) \quad V'_j = V'(p^j) = G(p^j)V(p^j)G(p^j)^T \quad (101)$$

4. Test closed-loop stability at iteration i using (102) for $j = 1, 2, \dots, M$. If any instability is found, go to 10.

$$\Phi_j(\mathcal{K}_i) = \Phi_j - \Gamma_j \mathcal{K}_i \quad C'_j = \Phi_j - \Gamma_j \mathcal{K}_i \quad G(p^j)C_j = \Phi_j - \Gamma_j K(p^j)C_j \quad (102)$$

5. Solve the P and S Lyapunov equations below for $j = 1, 2, \dots, M$

$$P_j(\mathcal{K}_i) = \Phi_j(\mathcal{K}_i)^T P_j(\mathcal{K}_i) \Phi_j(\mathcal{K}_i) + C'_j{}^T \mathcal{K}_i^T R_j \mathcal{K}_i C'_j + Q_j \quad (103)$$

$$S_j(\mathcal{K}_i) = \Phi_j(\mathcal{K}_i) S_j(\mathcal{K}_i) \Phi_j(\mathcal{K}_i)^T + \Gamma_j \mathcal{K}_i V'_j \mathcal{K}_i^T \Gamma_j^T + W_j \quad (104)$$

$$\hat{P}_j(\mathcal{K}_i) = \Gamma_j^T P_j(\mathcal{K}_i) \Gamma_j + R_j \quad (105)$$

$$\hat{S}_j(\mathcal{K}_i) = C'_j S_j(\mathcal{K}_i) C'_j{}^T + V'_j \quad (106)$$

6. Compute the cost $J'(\mathcal{K}_i)$ using (91) and (92 b). If the cost is not lower than last iteration, go to 10.

7. Compute the integrated/constrained gradient $j(\mathcal{K}_i)$ using (96) - (98). If the gradient norm is smaller than the convergence criterion, stop.

8. Solve for the variable-gain direction $d(\mathcal{K}_i)$ in

$$\sum_{j=1}^M f_j \hat{P}_j(\mathcal{K}_i) d(\mathcal{K}_i) \hat{S}_j(\mathcal{K}_i) = -j(\mathcal{K}_i) \quad (107)$$

If $M = 1$ (i.e., single model case), use Equation (75) to solve for the direction d .

If $M > 1$ (i.e., Multi-Model or Variable-Gain (V-G) cases), use the Kronecker product formulation given by (107 a).

$$\left[\sum_{j=1}^M f_j \left\{ \hat{S}_j(\mathcal{K}_i) \otimes \hat{P}_j(\mathcal{K}_i) \right\} \right] \text{col}\{d(\mathcal{K}_i)\} = -\text{col}\{j(\mathcal{K}_i)\} \quad (107 \text{ a})$$

where \otimes denotes the Kronecker product and col denotes the column vector form of the appropriate matrix. Solve for the direction by inverting the matrix in brackets or use the approximation algorithm described in Equations (74) - (81) in [5], pp.30-31.

9. Zero out the direction and go to 11.

$$d(\mathcal{K}_i) = d(\mathcal{K}_i) \times Z \quad (108)$$

10. Reduce step size α_i ; e.g.,

$$\alpha_{i+1} = \alpha_i / 2 \quad (109)$$

If step size is smaller than criterion, stop.

11. Compute new gain matrix and go to 4.

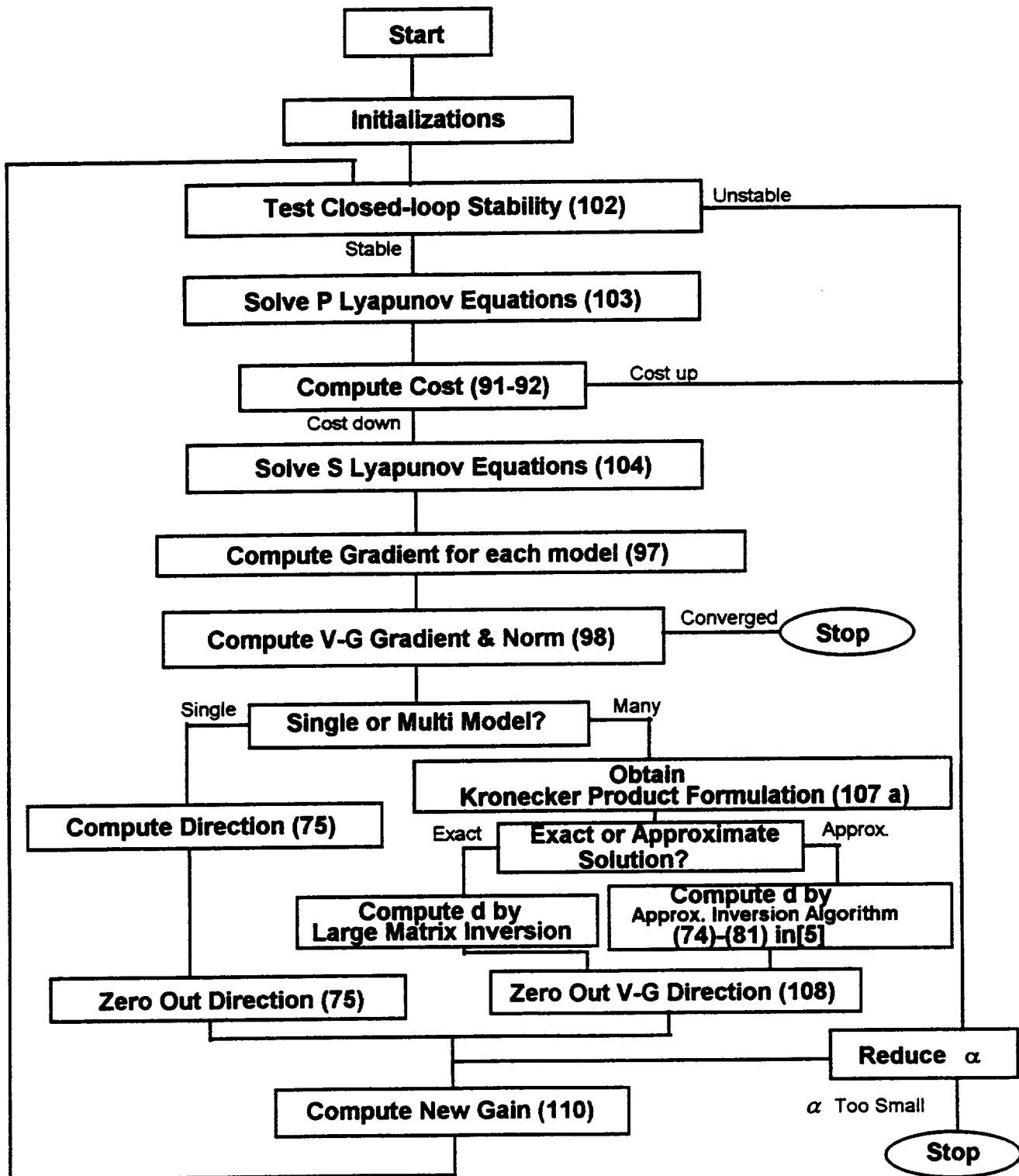
$$\mathcal{K}_{i+1} = \mathcal{K}_i + \alpha_i d(\mathcal{K}_i) \quad (110)$$

$$i \leftarrow i + 1 \quad (111)$$

The algorithm given above is intended for the Integrated/Constrained Variable-Gain Output Feedback Control problem. However, it also applies to the time-invariant or constant gain problem when the number of models, M , equals 1 and the dimension of the parameter vector, p , is also 1; i.e., $q = 0$. Furthermore, this algorithm is also applicable to the Multi-Configuration Control (MCC) problem described in [5].

Computing the direction in which to search for a lower cost is relatively straight-forward for single model problems as seen from (75). However, for multi-model problems (107) can be computationally demanding. An approximate solution can be obtained with significantly less computational burden by approximating the Hessian as shown in [5]. On the other hand, this may result in a more shallow direction for the search.

D. FLOW CHART OF VARIABLE-GAIN (V-G) ALGORITHM



IV. AN INTEGRATED FLIGHT AND PROPULSION CONTROL EXAMPLE

The Integrated SOFFT Control approach developed in the previous sections was applied to the design of an integrated flight and propulsion control system for the modified F-15 SMTD aircraft to provide an example of the design methodology developed. Although the methodology is applicable to both single model and multi-model variable-gain problems, here we will only design a single model control at one flight condition. Clearly, the Integrated SOFFT Control methodology is very general and has numerous applications in a variety of fields.

A. AIRFRAME AND PROPULSION MODELS

The modified F-15 SMTD aircraft model has an advanced propulsion system with thrust vectoring capability and has aerodynamic canards to complement the usual assortment of aerodynamic control surfaces. The aircraft has static instability in the longitudinal dynamics at a flight condition of 30 degrees of angle-of-attack. It is open-loop stable at the other high angle-of-attack flight conditions we have considered. Accordingly, we select the flight condition for 30 degrees angle-of-attack at level flight in order to observe the impact of the static instability on the methodology. From the results obtained in the investigation, the methodology stabilizes the open-loop unstable mode without any noticeable consequences.

The thrust vectoring can produce moments in the pitch, yaw and roll axes. Thus, it has three control components. These thrust vectoring components have very similar effects as the aerodynamic control surfaces, namely, the stabilator, rudder and ailerons. In normal operation, it would be counter-intuitive to command positive rolling moment with the

ailerons while simultaneously commanding negative rolling moment with thrust vectoring, thus canceling each other's effects. Accordingly, we select to combine the thrust vectoring controls with the corresponding aerodynamic control surfaces. This reduces the number of control components and reduces the computational load and avoids situations as the one mentioned above.

The aerodynamic surface and thrust vectoring controls are shown in Table 1.

Table 1. Airframe Controls				
$\delta =$	δ_s	degrees	Stabilator	+ pitch down
	δ_θ	degrees	Pitch Thrust Vectoring	+ pitch down
	δ_A	degrees	Aileron	+ roll right
	δ_R	degrees	Rudder	+ yaw left
	δ_ψ	degrees	Yaw Thrust Vectoring	+ yaw left
	δ_ϕ	degrees	Roll Thrust Vectoring	+ roll right

Let u_{x1} be the new or combined airframe control vector (having three components) which we will use in the plant model. Then the airframe controls in Table 1 are obtained as follows.

$$\delta = \begin{pmatrix} 1 & 0 & 0 \\ 1/2 & 0 & 0 \\ 0 & 1 & 0 \\ 0 & 0 & .6 \\ 0 & 0 & .9 \\ 0 & 1/2 & 0 \end{pmatrix} u_{x1} \quad u_{x1} = \begin{pmatrix} u_\theta \\ u_\phi \\ u_\psi \end{pmatrix} \quad (112)$$

The airframe state vector is given in Table 2.

Table 2. Airframe State Variables		
$x_1 =$	$\begin{pmatrix} V \\ \alpha \\ q \\ \theta \\ \beta \\ p \\ r \\ \phi \end{pmatrix}$	<i>ft / sec</i> <i>degrees</i> <i>deg / sec</i> <i>degrees</i> <i>degrees</i> <i>deg / sec</i> <i>deg / sec</i> <i>degrees</i> <i>speed along x_1</i> <i>angle of attack</i> <i>pitch rate</i> <i>pitch angle</i> <i>sideslip</i> <i>roll rate</i> <i>yaw rate</i> <i>roll angle</i>

In Table 2 and elsewhere, x_1 denotes the x stability axis. In a similar vein, the engine controls were combined from a total of five components to the following three.

Table 3. Propulsion Control Variables		
$u_{x2} =$	$\begin{pmatrix} WFP \oplus WFA \\ AJ \\ RCVV \end{pmatrix}$	<i>1,000 lbs / hr</i> <i>100 in²</i> <i>degrees</i> <i>Fuel Flow</i> <i>Exhaust Nozzle Area</i> <i>Rear Compressor Variable Vane</i>

The propulsion state vector and units are given in Table 4.

Table 4. Propulsion State Variables		
$x_2 = \begin{pmatrix} N_1 \\ N_2 \\ HPCT \end{pmatrix}$	1,000 rpm 1,000 rpm 1,000 R°	Low Rotor Speed High Rotor Speed Rear Compressor Metal Temperature

The state equations for the airframe and propulsion subsystems are of the form

$$\dot{x}_1 = A_1 x_1 + B_1 u_{x1} + B'_{11} u_{11} \quad (113)$$

$$\dot{x}_2 = A_2 x_2 + B_2 u_{x2} + B'_{22} u_{22} \quad (114)$$

The cross-coupling terms, the last terms in the equations above, are given by

$$u_{11} = \begin{pmatrix} F_g \\ D_p \end{pmatrix} \quad u_{22} = \begin{pmatrix} \alpha \\ \beta \end{pmatrix} \quad (115)$$

where F_g and D_p are the gross thrust and the drag due to the engine. Substituting for the cross-coupling terms and manipulating, the integrated continuous open-loop system can be found as

$$\dot{x}_1 = A_{x11} x_1 + A_{x12} x_2 + B_{x11} u_{x1} + B_{x12} u_{x2} \quad (116)$$

$$\dot{x}_2 = A_{x21} x_1 + A_{x22} x_2 + B_{x22} u_{x2} \quad (117)$$

The details of the derivation are given in Appendix B. It should be noted that several of the system matrices in (116) and (117) are different than the ones in (113) and (114) (See (B-8) and (B-9) in Appendix B). Also note that the propulsion subsystem dynamics in (117) do not have a term for the airframe controls although there is still some coupling through the state vector even if small.

The integrated system A_x and B_x matrices are shown in Tables 5 and 6, respectively.

Table 5. Integrated System A_x Matrix

	1	2	3	4	5
1	-0.2201	-0.6139	0.0000	-0.4532	-0.0274
2	-0.0801	-0.2040	1.0000	0.0630	0.0030
3	-0.0849	0.4817	-0.2448	0.0000	-0.0030
4	0.0000	0.0000	1.0000	0.0000	0.0000
5	0.0000	0.0000	0.0000	0.0000	-0.1251
6	0.0000	0.0000	0.0000	0.0000	-24.8180
7	0.0000	0.0000	0.0000	0.0000	-0.9008
8	0.0000	0.0000	0.0000	0.0000	0.0000
9	0.0000	0.0133	0.0000	0.0000	0.0136
10	0.0000	0.0076	0.0000	0.0000	0.0075
11	0.0000	0.0000	0.0000	0.0000	0.0000
	6	7	8	9	10
1	0.0000	0.0000	0.0000	0.6337	0.0804
2	0.0000	0.0000	0.0000	-0.0695	-0.0088
3	0.0000	0.0000	0.0000	0.0687	0.0087
4	0.0000	0.0000	0.0000	0.0000	0.0000
5	0.5000	-0.8660	0.1060	0.0000	0.0000
6	-0.7052	1.5406	0.0000	0.0000	0.0000
7	0.0150	-0.2254	0.0000	0.0000	0.0000
8	1.0000	-0.1086	0.0000	0.0000	0.0000
9	0.0000	0.0000	0.0000	-2.5764	1.7038
10	0.0000	0.0000	0.0000	0.0213	-1.5592
11	0.0000	0.0000	0.0000	0.0176	0.0149
	11				
1	0.2598				
2	-0.0285				
3	0.0281				
4	0.0000				
5	0.0000				
6	0.0000				
7	0.0000				
8	0.0000				
9	0.4365				
10	0.3440				
11	-0.3846				

Table 6. Integrated System B_x Matrix

	1	2	3	4	5
1	-0.4182	0.0000	0.0000	0.5901	-2.1013
2	-0.1326	0.0000	0.0000	-0.0647	0.2304
3	-3.4895	0.0000	0.0000	0.0639	-0.2277
4	0.0000	0.0000	0.0000	0.0000	0.0000
5	0.0000	0.0060	0.0813	0.0000	0.0000
6	0.0000	3.8394	0.0031	0.0000	0.0000
7	0.0000	-0.1895	-3.7094	0.0000	0.0000
8	0.0000	0.0000	0.0000	0.0000	0.0000
9	0.0000	0.0000	0.0000	0.9496	2.3631
10	0.0000	0.0000	0.0000	0.5476	0.7002
11	0.0000	0.0000	0.0000	0.0019	-0.0068
	6				
1	0.0015				
2	-0.0002				
3	0.0002				
4	0.0000				
5	0.0000				
6	0.0000				
7	0.0000				
8	0.0000				
9	0.2151				
10	-0.1431				
11	0.0009				

It should be noted here that the propulsion control vector and, therefore, the B_x matrix was modified for the final design example. This new control vector and the motivation for the change are described in the next section

Finally, the integrated system measurement or feedback vector was selected as shown in Table 7. Note that the first six measurements may be considered to be airframe measurements with the remaining four measurements corresponding to the propulsion system. However, both sets contain variables from the other subsystem.

Table 7. Integrated System Measurement/Feedback Variables

$y_x =$	a_x	ft/sec^2	<i>acceleration along x,</i>
	α	<i>degrees</i>	<i>angle of attack</i>
	q	<i>deg/sec</i>	<i>pitch rate</i>
	β	<i>degrees</i>	<i>sideslip angle</i>
	p	<i>deg/sec</i>	<i>roll rate</i>
	r	<i>deg/sec</i>	<i>yaw rate</i>
	N_1	<i>1,000 rpm</i>	<i>low rotor speed</i>
	N_2	<i>1,000 rpm</i>	<i>high rotor speed</i>
	$HPCT$	<i>1,000 R°</i>	<i>rear compressor metal temperature</i>
	$SMHC$	<i>%</i>	<i>rear compressor stall margin</i>

Finally, although we have treated the problem as one with two subsystems, namely the airframe and the propulsion subsystems, it is possible to consider it as a problem with three subsystems: the longitudinal airframe dynamics, the lateral airframe dynamics and the propulsion subsystems. In fact, the most common integrated control problem in flight controls certainly has to be the longitudinal and lateral flight control systems. Although usually treated separately, these two subsystems are coupled when the aircraft has a nonzero roll angle.

B. FEEDFORWARD CONTROL DEVELOPMENT

In this section, we will discuss the formulation and selection of the command model for the integrated system. However, most of the comments made here apply to centralized optimization problems as well. In particular, we will discuss the selection of the number of variables which should be commanded for best results in the next subsection.

1. Input Command Considerations

The first feedforward design question is the selection of the pilot input commands. This selection is often the one mentioned to describe the overall control system. For example, we will say that we have a "pitch rate command system" or an "alpha-command system" or an "attitude rate command system" meaning that the pilot commands those variables.

It is generally accepted that we can have as many commands as the number of independent control variables. While this may be true in a strict sense, it is not always the most reasonable or desirable number to select as we shall discuss in the following. Other considerations may lead the designer to select a different number of input commands.

From the integrated model described in the previous section, the overall system order is 11 and the number of controls is 6. Therefore, we started out by selecting 6 input commands. Not all of the commands need to be input by the pilot as real-time inputs. Some commands may be computed according to given formulas or algorithms. In other cases, some input commands may simply be constant commands.

Some examples of input command vectors are shown below.

$$H_y y_x^* = \begin{pmatrix} q + .2\alpha \\ a_x \\ p \\ r \\ SMF \\ SMHC \end{pmatrix}^* \quad \begin{pmatrix} q + .2\alpha \\ a_x \\ p \\ r \\ N_1 \\ N_2 \end{pmatrix}^* \quad \begin{pmatrix} q + .2\alpha \\ N_2 \\ p \\ r \\ SMF \\ SMHC \end{pmatrix}^* \quad (118)$$

All of the choices above resulted in very high cross-gain values from the longitudinal airframe state variables to the propulsion control variables. Several other selections were tried to eliminate various possible causes for such high gains. For example, decoupling the engine dynamics from the airframe by setting A_{x21} to zero produced no significant change. Decoupling the input command vector itself by commanding 3 airframe and 3 engine states helped to reduce the cross-gains somewhat. However, the gains from the engine

states to the engine controls were still high. The last result, coupled with the previous ones, pointed to a new approach to the problem.

Our hypothesis was that the reason the gains are very high is due to the possibility of commanding the three engine state variables (or an equivalent set of variables) to unreasonable, mutually opposing values. For example, it is possible to command N_1 to high rpm's and simultaneously command N_2 to lower rpm's while commanding HPCT to remain constant. The input command selections above make this a possibility even if such a command profile never actually occurs. Therefore, the control law must be able to achieve unrealistic commands. And it does! But at the expense of very high gains. Of course, the propulsion system is not designed to track such commands; it is designed to produce thrust, a single variable.

Thus, even though, strictly speaking, it is possible to command as many variables as the number of controls, it may be totally unreasonable to do so. One must take into account the characteristics of each subsystem before selecting the input command vector. **Just because it is possible to command many variables does not mean we are required to do so.** It is of interest to investigate further the conditions under which such situations occur. However, such an investigation is beyond the scope of the present study.

To prove the hypothesis above, we reformulate the propulsion problem as a one-control one-command problem. Consider the single component pseudo control u_c defined by

$$u_{x2} = G_2 u_c \quad (119)$$

where u_{x2} is the propulsion vector in Table 3 and G_2 is a 3×1 matrix to be determined. Let us choose G_2 so as to minimize the E-norm of the feedforward gain matrix K_x^* . After considerable work, it is possible to show that the minimum occurs for

$$G_2 = c \begin{pmatrix} 1.0 \\ 3.34 \\ 0.21 \end{pmatrix} \quad (120)$$

where c is a arbitrary scalar. We do not show the derivation here as it is not relevant to the problem under consideration. Suffice it to know that using this vector with c equal to

1, together with the input command vector shown below, immediately solved the problem of very high gains reducing K_x^* by several orders of magnitude. We consider the hypothesis proved heuristically by finding a solution which dramatically reduces the gain.

$$H_y y_x^* = \begin{pmatrix} q + .2\alpha \\ p \\ r \\ a_{xx} \end{pmatrix}^* \quad (121)$$

Accordingly, we select eq. (121) as the pilot input command vector for this example. However, minimizing the norm of the gain matrix is not necessarily the best way to select our pseudo control. In particular, the choice of (120) results in a negative value for the (1,4) element of B_x . Thus, a positive step in the pseudo control would produce an initial tendency to reduce the thrust and the forward acceleration. This tendency would reverse itself after the transient response dies down. To avoid this counter-intuitive initial tendency, we modified the value of G_2 as shown in (122) so that the pseudo control would produce the desired initial response without introducing large moments in the pitch rate (q) and angle-of-attack (α) equations. The resulting B_x matrix is shown in Table 8.

$$G_2 = \begin{pmatrix} 4 \\ 1 \\ 1 \end{pmatrix} \quad (122)$$

2. Command Model or Flying Qualities

Given the pilot input command vector, we need to select a command model which produces the flying qualities desired by the pilot. In the SOFFT methodology, the command model determines the response of the aircraft dynamics to the pilot's input commands. In this example, we select the command model to produce specific types of responses for each component of the vector in (121).

For the longitudinal and lateral dynamics, we will use [14], pp.511 - 525 as a guide in selecting the corresponding command models. For the propulsion related forward

Table 8. Integrated System Modified B_x Matrix

	1	2	3	4
1	-0.4182	0.0000	0.0000	0.2605
2	-0.1326	0.0000	0.0000	-0.0286
3	-3.4895	0.0000	0.0000	0.0282
4	0.0000	0.0000	0.0000	0.0000
5	0.0000	0.0060	0.0813	0.0000
6	0.0000	3.8394	0.0031	0.0000
7	0.0000	-0.1895	-3.7094	0.0000
8	0.0000	0.0000	0.0000	0.0000
9	0.0000	0.0000	0.0000	6.3768
10	0.0000	0.0000	0.0000	2.7474
11	0.0000	0.0000	0.0000	0.0016

acceleration dynamics, it is not clear that a flying quality criterion is available. Accordingly, we will select a first order model for this variable.

Note that the command model dynamics can be varied in real time as the parameter vector follows the aircraft's flight condition for the variable-gain case. Thus, different flying qualities can be obtained at different flight conditions. We should point out that the command model selected here is not intended as a recommendation for flying qualities, but only as an example for use in demonstrating the Integrated SOFFT control methodology developed. With the advent of advanced aircraft with significantly different airframe components and new propulsion systems, the question of what flying qualities are most appropriate is itself a subject of research.

We will specify the command model for each component of the pilot input command vector as a continuous transfer function. These will be put into state variable form and discretized to obtain the command model in the form shown in (6) and (7) for the sampled-data control problem at hand.

$$\frac{y_{z1}(s)}{u_{z1}} = \frac{\omega_q^2}{s^2 + 2\zeta_q\omega_q s + \omega_q^2}, \quad \omega_q = 3, \zeta_q = .7 \quad (123)$$

$$\frac{y_{z2}(s)}{u_{z2}} = \frac{\omega_p^2}{s^2 + 2\zeta_p \omega_p s + \omega_p^2}, \quad \omega_p = 3, \zeta_p = .7 \quad (124)$$

$$\frac{y_{z3}(s)}{u_{z3}} = \frac{1}{\tau_r s + 1}, \quad \tau_r = 1.5 \quad (125)$$

$$\frac{y_{z4}(s)}{u_{z4}} = \frac{1}{\tau_a s + 1}, \quad \tau_a = 1 \quad (126)$$

3. Feedforward Control Gain Matrices

With the integrated model given in (116) and (117), the pilot input command vector given in (121) and the command model given in (123) - (126), we can design the feedforward control law as described in Section II.A.1. Of course, the integrated system and command model were first discretized using the standard sampled-data discretization methods and the control-dependent measurement augmentation shown in (42) and (43) was applied to the integrated system before actually computing the feedforward gain matrices.

Note that, the system augmentation due to the control-dependent measurements increases the order of the integrated system from 11 to 13. As only two of the control components are used in the measurements, we only need to augment the integrated state by those two components. The feedforward control has the form (also see Fig 3, p.16)

$$u_{xk}^* = -K_x^* x_k^* - K_z z_k - K_{uz} u_{zk} \quad (10)$$

Using the perfect tracking feedforward control case, the three gain matrices in (10) were computed according to equations (11) - (13). These gain matrices are shown in Tables 9, 10 and 11.

Table 9. Feedforward Control Gain Matrix : K_x^*

u_k^*	V_k^*	α_k^*	q_k^*	θ_k^*	β_k^*
u_θ^*	0.0248	-1.5723	-7.1625	-0.0128	0.0001
u_ϕ^*	0.0000	0.0000	0.0000	0.0000	-6.4473
u_ψ^*	0.0000	0.0000	0.0000	0.0000	0.5715
u_δ^*	-0.4874	-2.9462	-7.0169	-1.0784	-0.0632
u_k^*	p_k^*	r_k^*	ϕ_k^*	N_{1k}^*	N_{2k}^*
u_θ^*	0.0000	0.0000	0.0000	-0.0033	-0.0001
u_ϕ^*	6.3787	0.2085	-0.0138	0.0000	0.0000
u_ψ^*	-0.3263	-6.7200	0.0012	0.0000	0.0000
u_δ^*	-0.0006	-0.0003	-0.0003	1.3406	0.2716
u_k^*	$HPCT_k^*$	u_{ak-1}^*	u_{ek-1}^*		
u_θ^*	-0.0011	0.0000	0.0000		
u_ϕ^*	0.0000	0.0000	0.0000		
u_ψ^*	0.0000	0.0000	0.0000		
u_δ^*	0.6279	-0.0003	0.0002		

Table 10. Feedforward Control Gain Matrix : K_z

u_k^*	z_1	z_2	z_3	z_4	z_5
u_θ^*	7.1230	0.2634	0.0000	0.0000	0.0000
u_ϕ^*	0.0000	0.0000	-6.5824	-0.2434	0.2978
u_ψ^*	0.0000	0.0000	0.3351	0.0124	6.5727
u_δ^*	6.8791	0.2544	-0.0007	0.0000	0.0025
u_k^*	z_6				
u_θ^*	-0.0187				
u_ϕ^*	0.0000				
u_ψ^*	0.0000				
u_δ^*	-2.2904				

Table 11. Feedforward Control Gain Matrix : K_{uz}

u_k^*	u_{z1}	u_{z2}	u_{z3}	u_{z4}
u_θ^*	0.0488	0.0000	0.0000	-0.0008
u_ϕ^*	0.0000	-0.0451	0.0080	0.0000
u_ψ^*	0.0000	0.0023	0.1776	0.0000
u_δ^*	0.0471	0.0000	0.0001	-0.0935

Some Important Observations

In the Integrated SOFFT Control methodology we have developed in this study, much of the "integration" is done by the feedforward control law since we have chosen to have the feedforward control law be centralized while the feedback is more limited in its cross-coupling. The feedback control law also performs important integration functions. However, the feedforward, not being constrained, is free to produce coupling as it finds necessary. Therefore, we may learn about which subsystems and which variables would be coupled if we did not have constraints.

With these thoughts in mind, observe the feedforward gain matrices for particular coupling trends. In K_x^* , note that the elements in the first row, on columns 9, 10, 11, have very small values. These elements correspond to the coupling from the propulsion system to the longitudinal dynamics subsystem. Clearly, the SOFFT feedforward does not produce much coupling from the propulsion to longitudinal subsystems.

On the other hand, the 4th row elements on columns 1 -4 do not have negligibly small values. These terms correspond to the coupling from the longitudinal dynamics to the propulsion subsystem. **In other words, the SOFFT feedforward uses longitudinal information in propulsion, but does not use the propulsion state in the longitudinal control.** Also note that, with the possible exception of the sidelip term $K_x^*(4,5)$, there is little coupling from the lateral dynamics to the propulsion subsystem. As would be expected in level flight, the lateral control does not use information from any other subsystem.

K_{ω} produces a leading control movement when the pilot moves his commands. Note that when an acceleration command is given, the initial control will be to increase the thrust through the propulsive control. However, only a small amount of stabilator control is used to maintain the pitch rate from moving. However, when a pitch rate command (with no acceleration command) is given, both the stabilator (with pitch thrust vectoring) and the propulsion control move in a coupled manner.

While these observations are often what an experienced designer might expect, it appears that the SOFFT feedforward control gain matrices contain important information as to which subsystems need coupling and maybe how much coupling. It is always a good idea to verify one's intuition with more objective methods.

C. FEEDBACK CONTROL DEVELOPMENT

With the feedforward control obtained, we can follow the development in Section II.A.1 and Section III to design a feedback control law for the integrated/constrained flight and propulsion control system. A Proportional-Integral-Filter (PIF) feedback control law was designed. The structure of the feedback law is as described in Section II.A.1. We show the relevant equations here for convenience.

$$\tilde{u}_{xk+1} = \tilde{u}_{xk} + \Delta t \tilde{v}_{xk} + w_{uk} \quad (19)$$

$$\tilde{I}_{k+1} = \tilde{I}_k + \Delta t (H_y \tilde{y}_{xk} + H_u \tilde{u}_{xk}) + w_{Ik} \quad (20)$$

With the control vector having 4 components and the integral feedback vector having 4 components as well, the system state is augmented from 13 to 21. Accordingly, the feedback vector consisting of the 10 measurements together with the 4 controls and 4 integrators is augmented to a dimension of 18.

The sampling rate used for sampling the sensor outputs and for updating the control commands is 25 Hz corresponding to a sampling period of 0.04 sec. The integral error feedback is obtained by using (121) to select the state components in the integral (more correctly, the accumulator). The control component of the integral is determined by H_u .

$$H_u = \begin{pmatrix} 0 & 0 & 0 & 0 \\ 0 & .05 & 0 & 0 \\ 0 & 0 & .05 & 0 \\ 0 & 0 & 0 & .05 \end{pmatrix} \quad (127)$$

The reason for using any control at all in the integrators is due to problems encountered in obtaining an initial stabilizing gain when the integrator produces a double eigenvalue in the system. For example, if the roll rate error is integrated for feedback, the integrator state is closely related to the roll angle component of the state. These conditions place at least numerical difficulties on the algorithms used. We have found, by experience, that adding a small amount of the corresponding control into the integrator differentiates it sufficiently to make the numerical problems disappear. We are not aware of a theoretical reason for

this condition. Presumably, an algorithm specifically designed to handle multiple eigenvalues would not run into the same difficulties. However, we have never tried to test this hypothesis.

The form of the control is given by (50) and (51) which we repeat here for convenience.

$$\tilde{v}_k = -K \tilde{Y}_k = - \begin{pmatrix} K_x & K_u & K_I \end{pmatrix} \begin{pmatrix} \tilde{y}_{xk} \\ \tilde{u}_{xk} \\ \tilde{I}_k \end{pmatrix} \quad (50)$$

$$\begin{pmatrix} \tilde{v}_{x1k} \\ \tilde{v}_{x2k} \\ \vdots \\ \tilde{v}_{xLk} \end{pmatrix} = - \left(\begin{array}{ccc|ccc|ccc} K_{x11} & \cdots & K_{x1L} & K_{u11} & \cdots & K_{u1L} & K_{I11} & \cdots & K_{I1L} \\ K_{x21} & \ddots & \vdots & K_{u21} & \ddots & \vdots & K_{I21} & \ddots & \vdots \\ \vdots & & & \vdots & & & \vdots & & \\ K_{xL1} & \cdots & K_{xLL} & K_{uL1} & \cdots & K_{uLL} & K_{IL1} & \cdots & K_{ILL} \end{array} \right) \begin{pmatrix} \tilde{y}_{x1k} \\ \vdots \\ \tilde{y}_{xLk} \\ \tilde{u}_{x1k} \\ \vdots \\ \tilde{I}_{1k} \\ \vdots \end{pmatrix} \quad (51)$$

Recall that K_{xij} , K_{uij} and K_{Iij} are dimensioned $n_{u_i} \times n_{y_j}$, $n_{u_i} \times n_{u_j}$ and $n_{u_i} \times n_{I_j}$, resp.. As mentioned before, with 4 control components and 18 feedback variables, the integrated feedback gain matrix has the dimensions of 4×18. The first 10 feedback variables are the measurements obtained from the sensors as shown in Table 7. The next 4 components are the control commands and the remaining 4 are the integrators.

1. Feedback Constraints

The considerations discussed at the end of Section IV.B.3 "Some Important Observations", can now provide some helpful hints as to how to select the constraints on feedback coupling of the subsystems. Accordingly, we first constrain the lateral controls to use only lateral variables for feedback. Then, with the exception of the sideslip angle, we constrain the propulsion and the longitudinal subsystems from using lateral feedback variables; i.e., measurements, controls or integrators. We allow the sideslip coupling because it is an input into the propulsion open-loop system. Accordingly, there already is

some coupling present. We are not really increasing the complexity of the closed-loop system by allowing further coupling. Only the extent of coupling may change.

Finally, we constrain the longitudinal control from using the propulsion measurements of HPCT and SMHC. However, we allow the use of the low and high rotor rpm's, N_1 and N_2 , in the measurements, largely as an experiment, to see if it will have an impact. We did not see any important impact and would not recommend this coupling in general.

With the exception of the lateral feedback variables, the propulsion subsystem control was not constrained. Table 12 shows the constraint matrix, Z , used in the optimization of the feedback control gain matrix.

Table 12. Constraint (Zero) Matrix : Z

	a_x	α	q	β	p
u_θ	1.0000	1.0000	1.0000	1.0000	0.0000
u_ϕ	0.0000	0.0000	0.0000	1.0000	1.0000
u_ψ	0.0000	0.0000	0.0000	1.0000	1.0000
u_e	1.0000	1.0000	1.0000	1.0000	0.0000
	r	N_1	N_2	HPCT	SMHC
u_θ	0.0000	1.0000	1.0000	0.0000	0.0000
u_ϕ	1.0000	0.0000	0.0000	0.0000	0.0000
u_ψ	1.0000	0.0000	0.0000	0.0000	0.0000
u_e	0.0000	1.0000	1.0000	1.0000	1.0000
	u_θ	u_ϕ	u_ψ	u_e	I_q
u_θ	1.0000	0.0000	0.0000	1.0000	1.0000
u_ϕ	0.0000	1.0000	1.0000	0.0000	0.0000
u_ψ	0.0000	1.0000	1.0000	0.0000	0.0000
u_e	1.0000	0.0000	0.0000	1.0000	1.0000
	I_p	I_r	I_{a_x}		
u_θ	0.0000	0.0000	1.0000		
u_ϕ	1.0000	1.0000	0.0000		
u_ψ	1.0000	1.0000	0.0000		
u_e	0.0000	0.0000	1.0000		

2. Feedback Gain Matrix

Using the algorithm developed in this work for the Integrated/Constrained Output Feedback Control problem, we computed the optimal feedback gain matrix. After some

trial-and-error experimentation, the gain matrix shown in Table 13 was computed. Simple observation indicates that the algorithm placed zero gain values at the appropriate locations specified by the constraint matrix.

Table 13. Constrained Feedback Gain Matrix : K					
	a_{xx}	α	q	β	p
u_θ	-3.4588	-21.9572	-13.8515	-0.0042	0.0000
u_ϕ	0.0000	0.0000	0.0000	-67.4612	11.3506
u_ψ	0.0000	0.0000	0.0000	7.1143	0.7541
u_r	0.4146	-2.2134	-1.4035	-0.1674	0.0000
	r	N_1	N_2	$HPCT$	$SMHC$
u_θ	0.0000	-0.2679	-0.6348	0.0000	0.0000
u_ϕ	5.1052	0.0000	0.0000	0.0000	0.0000
u_ψ	-9.2444	0.0000	0.0000	0.0000	0.0000
u_r	0.0000	2.5412	1.4876	2.1020	0.1145
	u_θ	u_ϕ	u_ψ	u_r	I_q
u_θ	10.6735	0.0000	0.0000	2.4268	-6.7740
u_ϕ	0.0000	12.4872	2.9060	0.0000	0.0000
u_ψ	0.0000	0.6132	12.5980	0.0000	0.0000
u_r	0.5549	0.0000	0.0000	8.0908	-1.8906
	I_p	I_r	$I_{a_{xx}}$		
u_θ	0.0000	0.0000	0.4299		
u_ϕ	14.1108	-1.4198	0.0000		
u_ψ	2.2957	-3.1476	0.0000		
u_r	0.0000	0.0000	8.5901		

The constrained feedback gain matrix provides the desired simplicity and other characteristics. However, an interesting question is whether the optimal gain matrix would not result in pretty much the same matrix as the one computed if we had not placed all the constraints. After all, the lateral dynamics are uncoupled from the longitudinal and propulsion subsystems. In other words, maybe we can achieve approximately the same result without as much work. Table 14 shows the feedback gain matrix obtained by optimizing the same cost function without any constraints.

As can be seen from Table 14, the unconstrained feedback gain matrix is highly coupled. In fact, the coupling seems to be present in all the subsystems. It is surprising to find the extent to which the lateral dynamics is now coupled with the other subsystems. Clearly,

the new approach and algorithm are necessary if we want to obtain an integrated/constrained feedback control law.

Table 14. Unconstrained Feedback Gain Matrix : K

	a_w	α	q	β	p
u_θ	-2.1948	-21.8214	-13.8979	1.3406	2.4836
u_ϕ	1.0281	1.2752	-1.0107	-56.0643	20.0745
u_ψ	0.3207	0.3319	0.1278	6.0044	0.2203
u_z	0.1629	-2.9952	-1.4927	-2.2007	-4.5740
	r	N_1	N_2	$HPCT$	$SMHC$
u_θ	-0.1072	-0.9778	-0.2175	0.2034	0.2427
u_ϕ	5.8336	-4.3872	-6.7735	-4.8243	13.5707
u_ψ	-9.2235	0.0733	0.6210	0.3184	-1.4593
u_z	0.0168	2.7710	1.5883	2.8411	0.8239
	u_θ	u_ϕ	u_ψ	u_z	I_q
u_θ	11.5028	0.4778	1.1337	1.3328	-6.4635
u_ϕ	4.3741	12.2794	3.1801	-28.6426	3.2624
u_ψ	-0.0300	0.7203	12.6883	1.6995	-0.0859
u_z	-0.3811	-0.4167	-0.6839	14.6445	-2.4864
	I_p	I_r	I_{a_w}		
u_θ	4.0241	-1.2069	-0.6368		
u_ϕ	23.5896	-4.4386	-22.8120		
u_ψ	1.6205	-3.2986	1.2380		
u_z	-4.5364	1.2960	11.9095		

D. SIMULATION RESULTS

A digital simulation of the integrated/constrained SOFFT control law obtained in the preceding sections together with the combined dynamics of the modified F-15 SMTD aircraft was developed on the ACET software package. The simulation of the modified F-15 SMTD aircraft was at the flight condition of 30 degrees of angle-of-attack in level flight. The integrated/constrained SOFFT control law was simulated in the incremental implementation form (see [1], [2] and Appendix A).

Two cases were simulated. At first, the simulated plant model was the one used in the feedforward control design. In the second case, the simulated plant B_x matrix was 10%

smaller than the control design model. In both cases, the simulation introduced no random plant or measurement noise into the system.

Figure 4 shows the results of the first simulation. This case did not provide a challenge for the feedback control law. However, we can see the feedforward control law producing the necessary control activity to track the pilot input commands and produce the response specified by the command model. In Figure 4a, we see that the pilot inputs are commanding an acceleration in the speed of the aircraft at the rate of 6ft/sec/sec for a period of 4 seconds and a simultaneous negative pitch rate plus angle-of-attack of -5 deg/sec for 3 seconds. These pilot input commands have been simulated as pulses or steps that last a finite period of time. Also note that the ACET simulation module automatically generates the y-axis labels which correspond to the variables plotted; e.g., UZ(4) is the fourth component of u_x , or the pilot input command of a_{x3} , YX(3) is the third component of y_x or the pitch rate, etc.

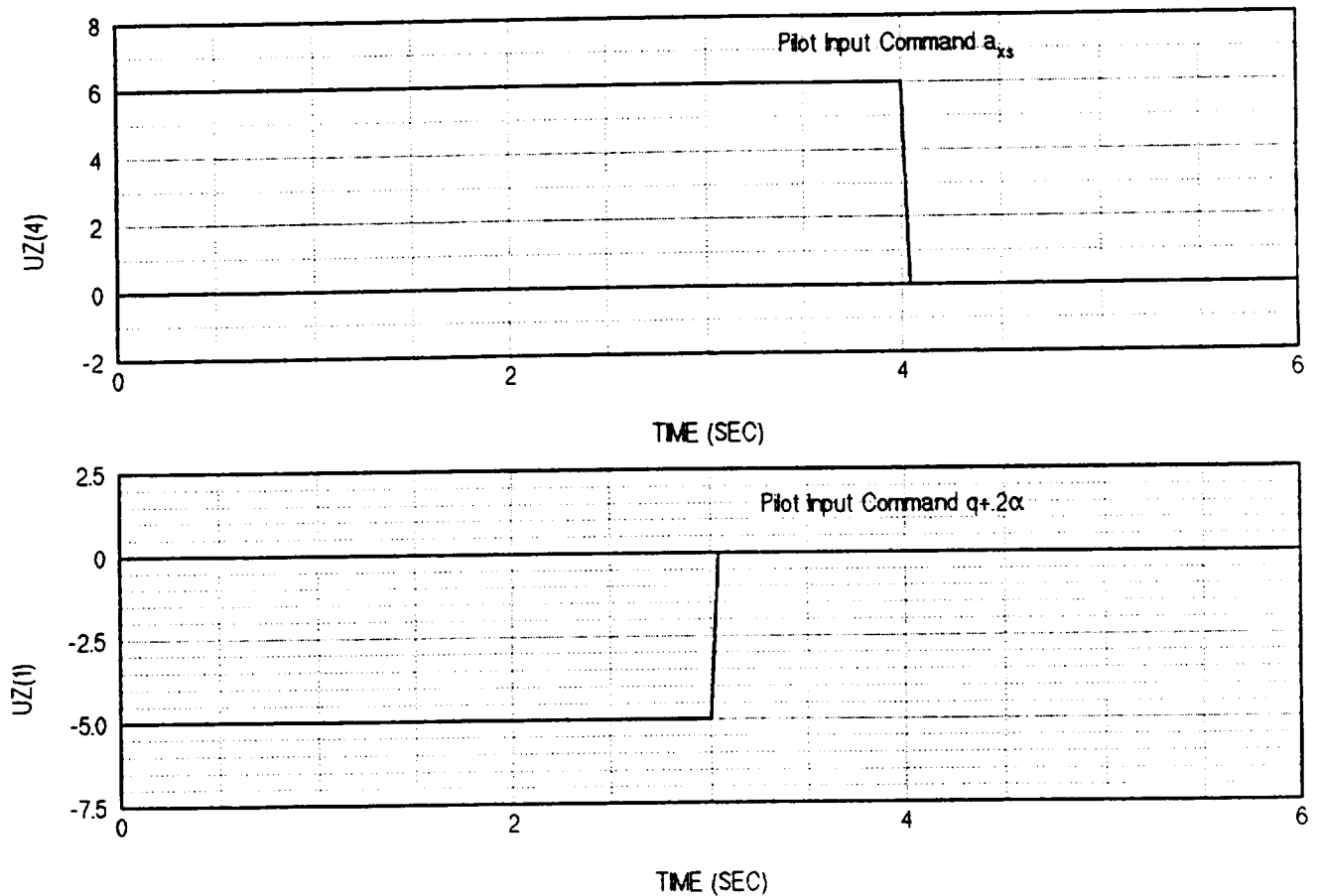


Figure 4a. Modified F-15 SMTD Integrated SOFFT Control Simulation, $\alpha=30^\circ$,
Pilot Input Commands

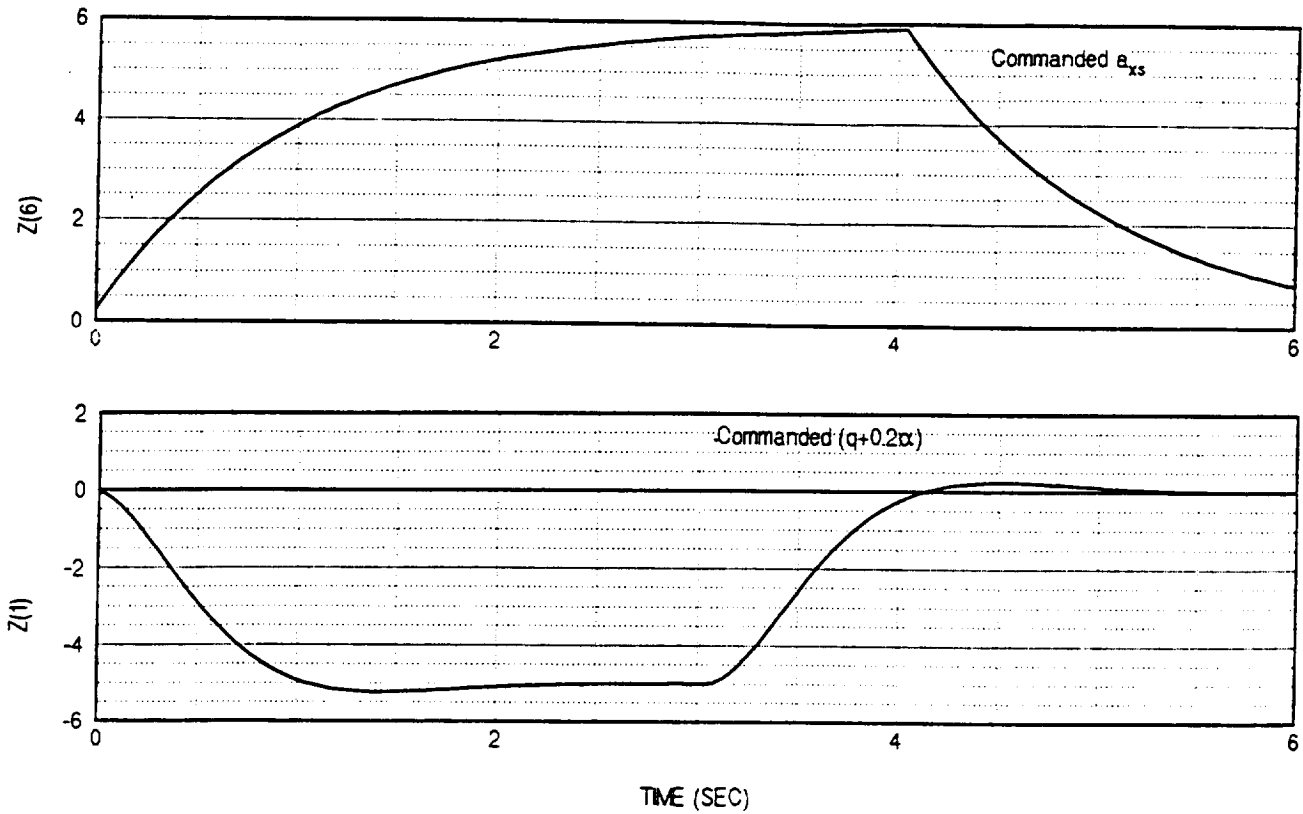


Figure 4b. Modified F-15 SMTD Integrated SOFFT Control Simulation, $\alpha=30^\circ$,
Command Model Outputs

Figure 4b shows the nonzero command model state variables (z_k) which correspond to the flying quality commands for the first and fourth elements in eq (121). Note that these represent the desired response of the aircraft to the input commands.

In Figure 4c, we see the response of the airframe variables to these commands. The acceleration tracks the commands with high accuracy. The pitch rate has a similar but somewhat different response than the command model output. The reason is that the command applies to the linear combination of the pitch rate and angle-of-attack.

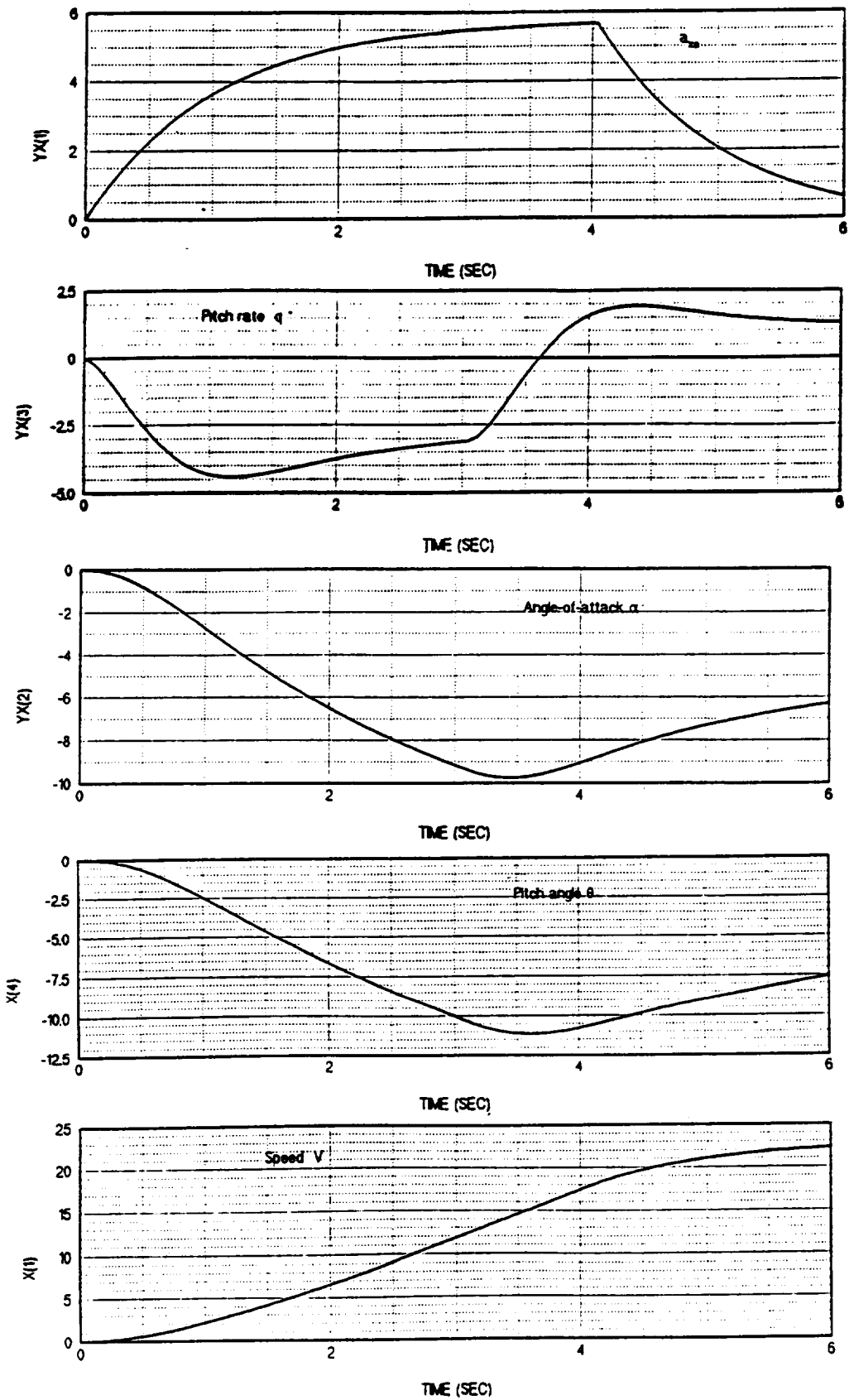


Figure 4c. Modified F-15 SMTD Integrated SOFFT Control Simulation, $\alpha=30^\circ$,
Airframe Variables

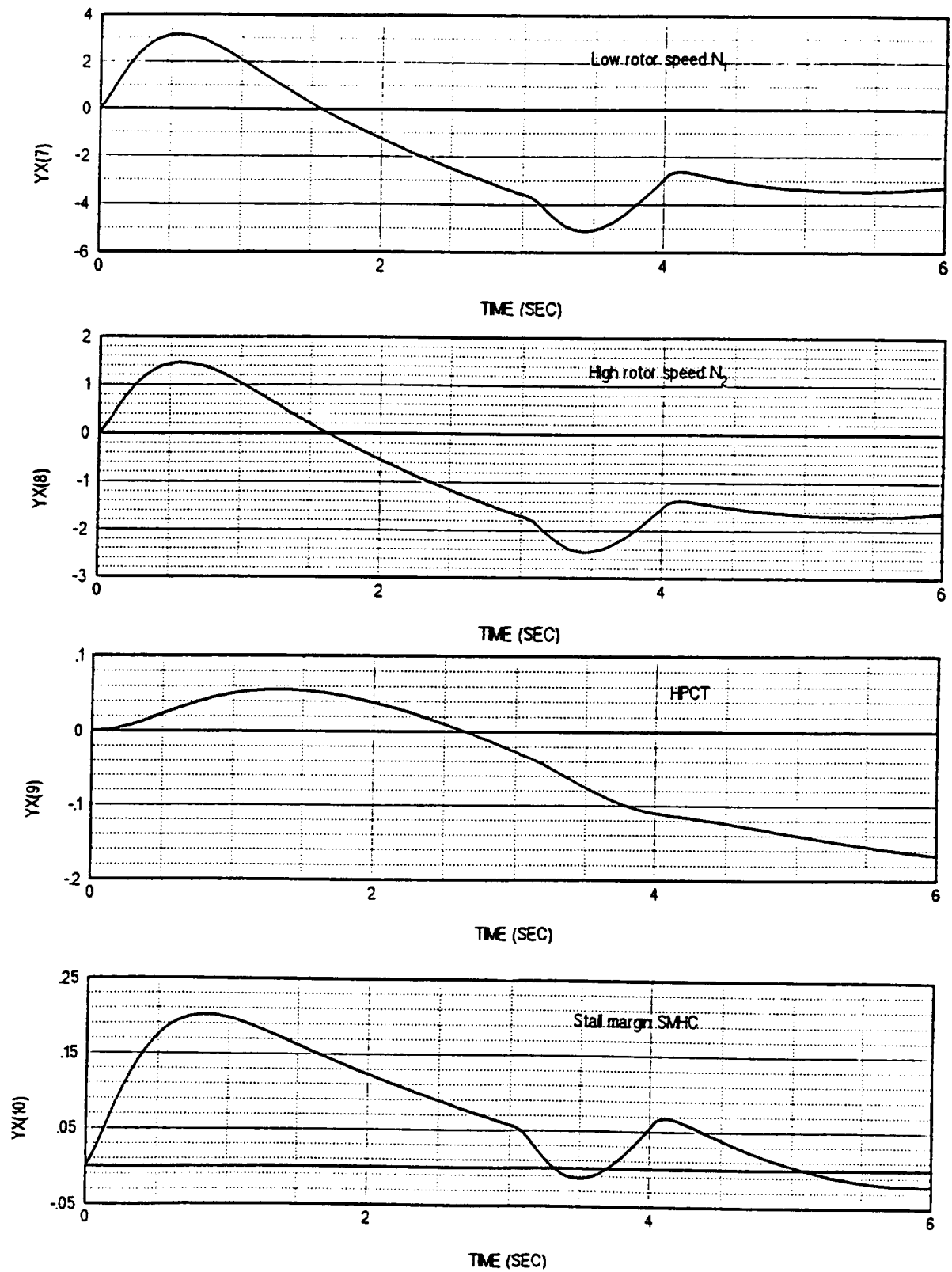


Figure 4d. Modified F-15 SMTD Integrated SOFFT Control Simulation, $\alpha=30^\circ$,
Propulsion Variables

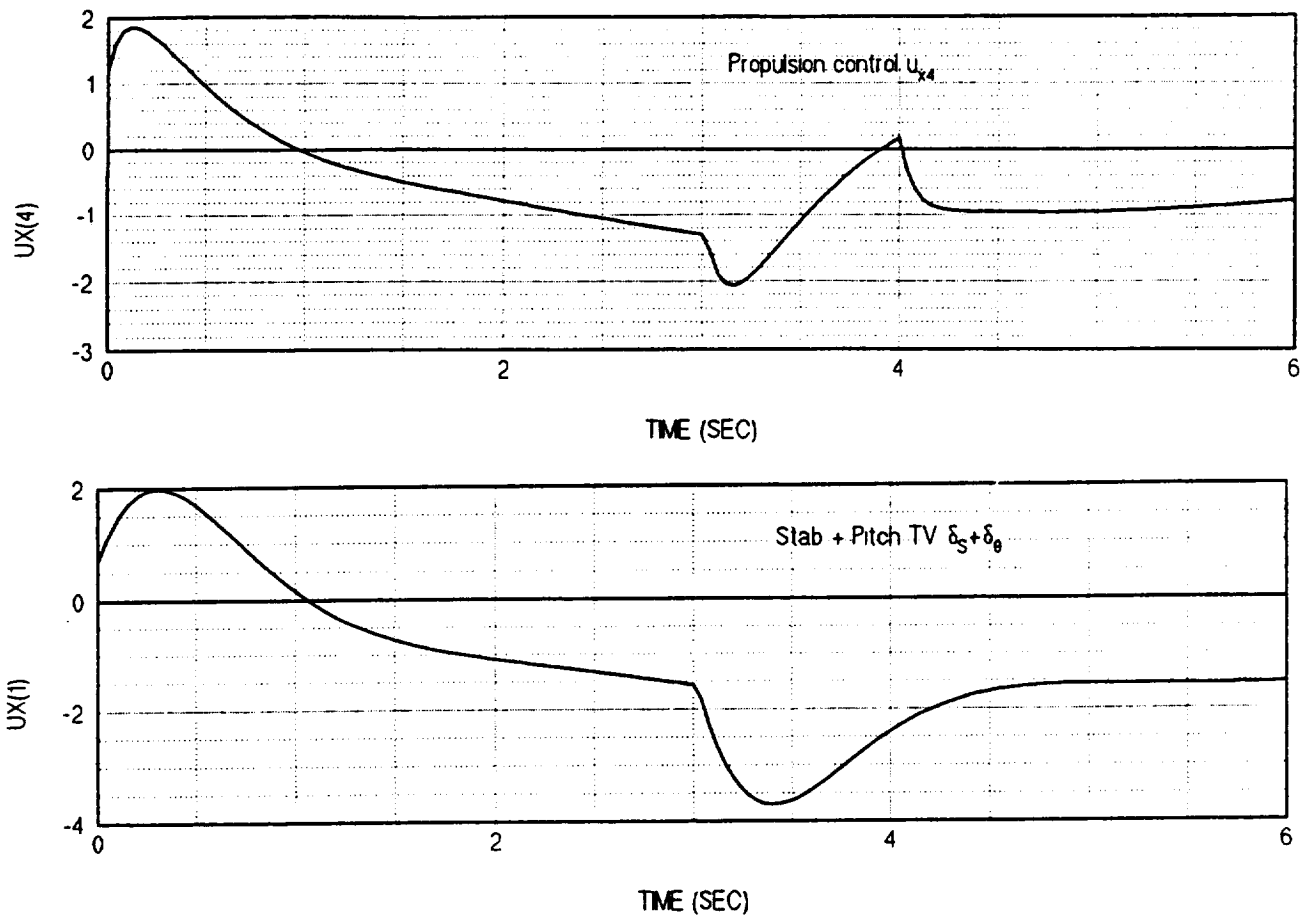


Figure 4e. Modified F-15 SMTD Integrated SOFFT Control Simulation, $\alpha=30^\circ$,
Control Variables

As the pitch angle and the angle-of-attack fall, the aircraft picks up speed from the combined effects of the pitch action reducing the drag and the initial increase in thrust.

The propulsion variables shown in Figure 4d first increase to produce more thrust needed to accelerate, but then fall to lower levels to avoid producing too much acceleration at the new angle-of-attack. Note that the stall margin remains in positive territory most of the time; i.e., it remains higher than its original comfortable level.

Finally, note the coordinated action of the propulsion and pitch controls shown in Figure 4e. Both controls move when the pitch rate command pulse input by the pilot ends at 3

seconds. On the other hand, when the acceleration pulse ends at 4 seconds, we see a reaction only in the propulsion control. This behaviour seems completely in line with our previous analysis of the feedforward gain matrices. Since the simulated plant and the design plant model are the same, the feedforward control produces the perfect response desired and the feedback control is null because the feedback state error is zero.

Figure 5 shows the simulation results for the second case considered. In this case, the simulated plant is different than the one used in designing the feedforward and feedback control laws. Accordingly, the feedforward control results in a state trajectory which is almost perfect but not exactly the same as the desired response. Therefore, the feedback state vector, the difference between the actual and feedforward states, is not zero. As a result the feedback control law tries to minimize the error by appropriate action.

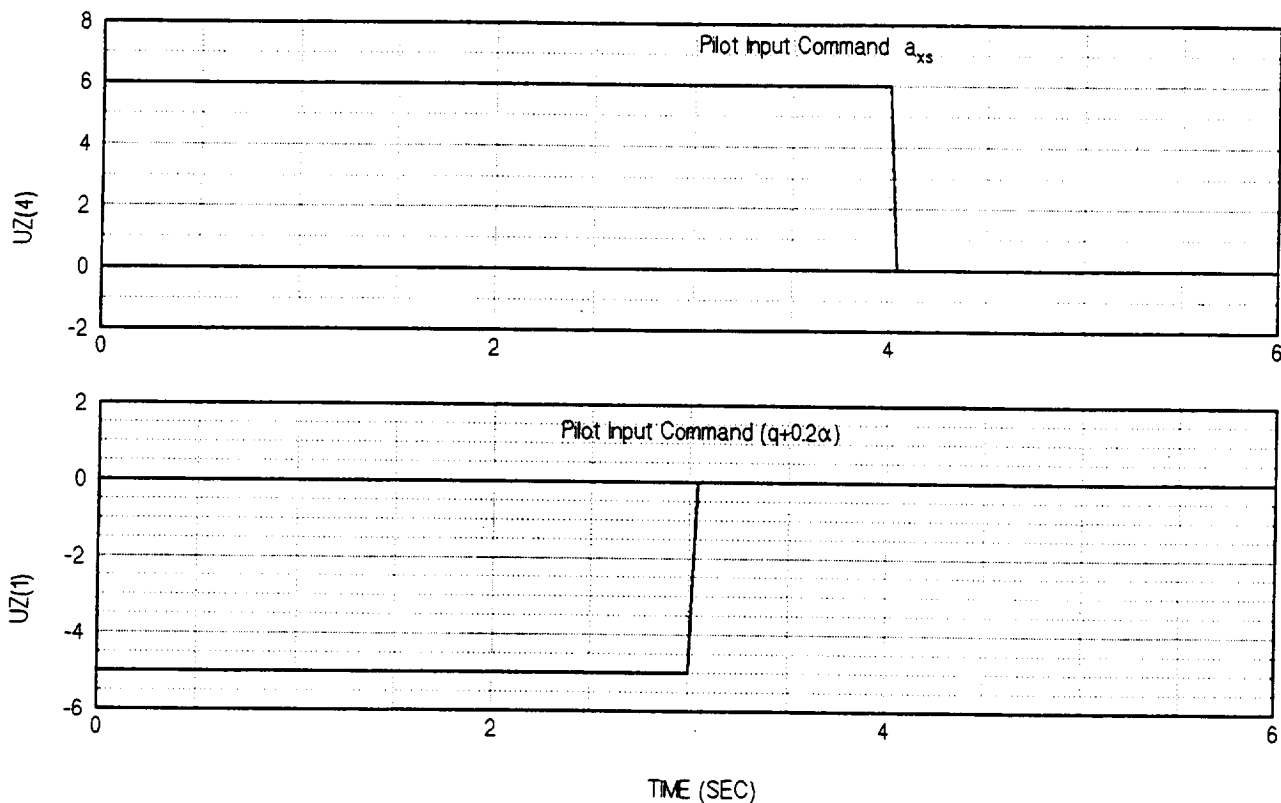


Figure 5a. Modified F-15 SMTD Integrated SOFFT Control Simulation, Perturbed Plant
Pilot Input Commands

As seen in Figure 5a, the pilot inputs are the same as the in the first case. The pilot commands an acceleration in the forward speed and a negative pitch rate action. It may be of interest to note that the feedforward control, which (by design) depends only on the input commands, will be the same as the first case since the design plant model has not changed. Recall that the simulated plant model has been perturbed, but the control design models have remained the same.

Figure 5b shows the relevant command model state variables generated in response to the pilot input commands. Since the command model has not changed, the input commands produce the same desired response as the first case.

In Figure 5c, we see some of the airframe variables. As noted earlier, since the control laws have been designed using an erroneous plant model, the state variables are not going to be perfect replicas of the desired response. On close observation, we can see that the forward acceleration is slightly different than the commanded acceleration in Figure 5b. However, the overall response is quite similar. It is harder to notice the differences in the pitch rate. Comparing the pitch rate and angle-of-attack to the desired response shown in Figure 4c, any offsets are hard to see.

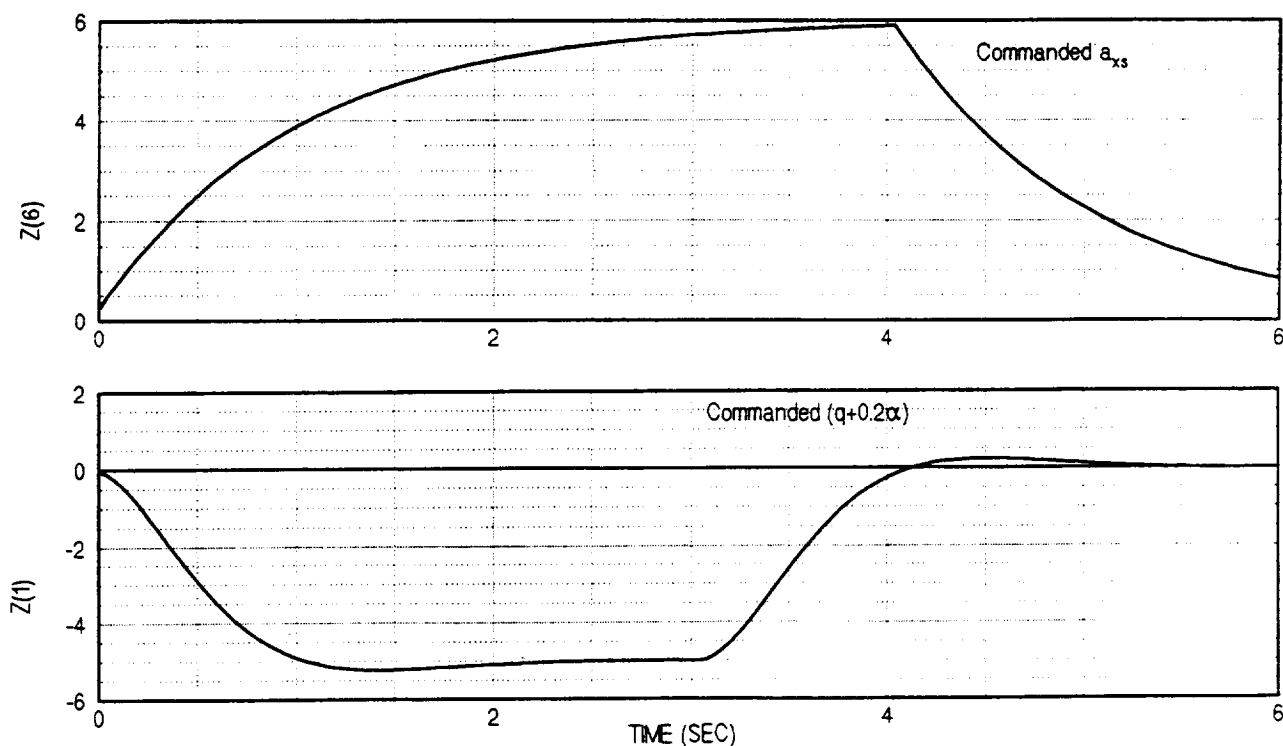


Figure 5b. Modified F-15 SMTD Integrated SOFFT Control Simulation, Perturbed Plant Command Model Outputs

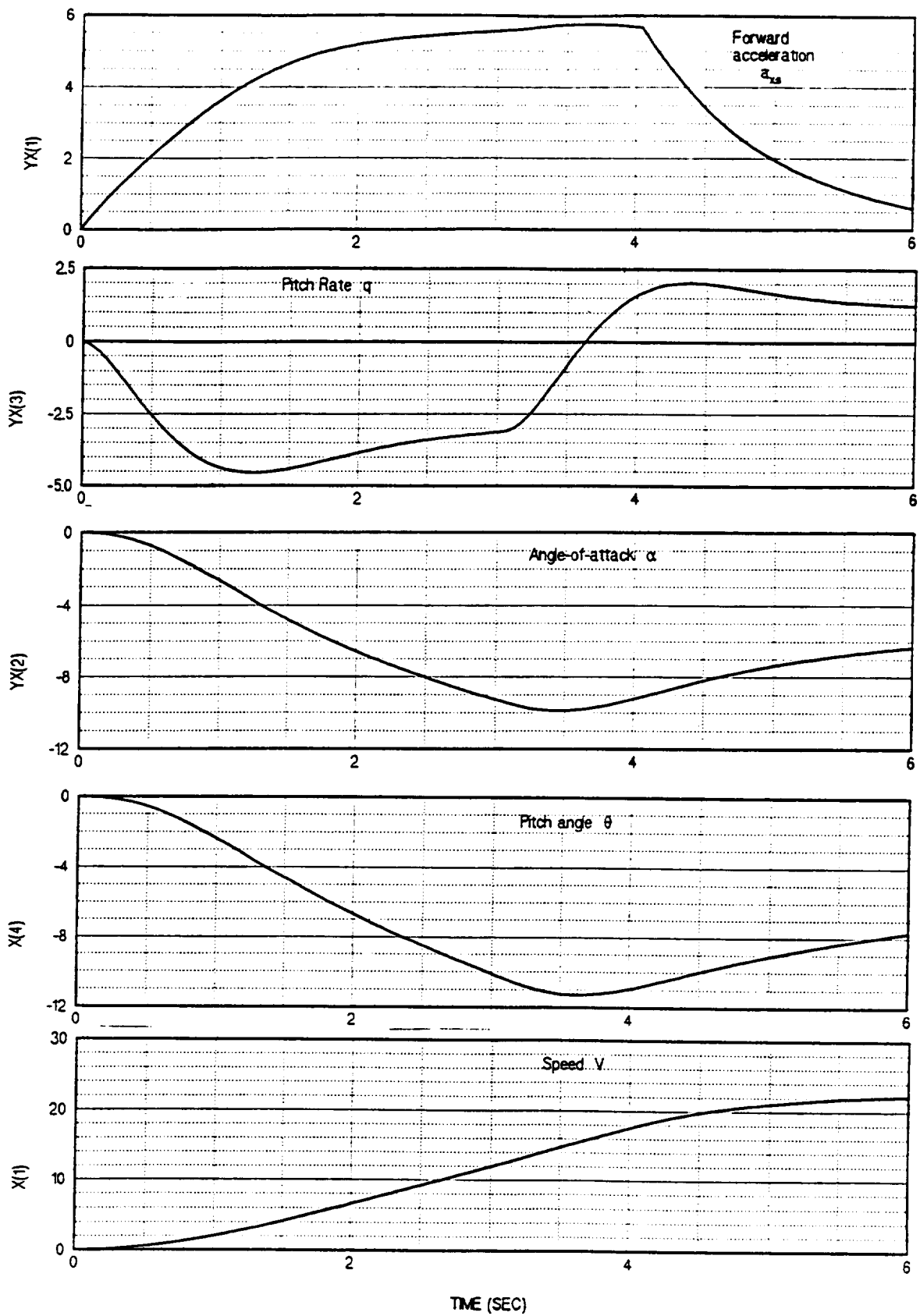


Figure 5c. Modified F-15 SMTD Integrated SOFFT Control Simulation, Perturbed Plant
Airframe Variables

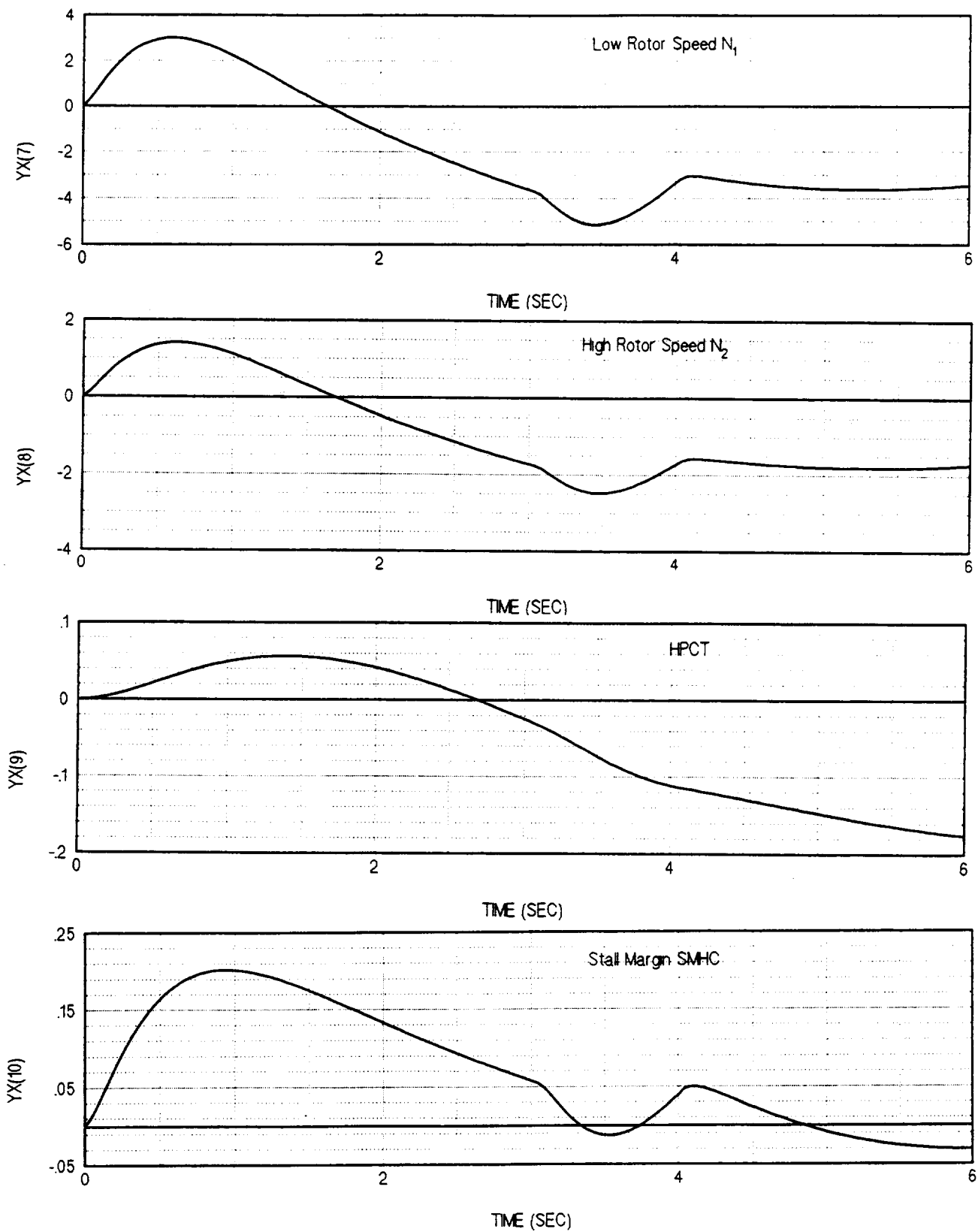


Figure 5d. Modified F-15 SMTD Integrated SOFFT Control Simulation, Perturbed Plant Propulsion Variables

Figure 5d shows the propulsion variables. Differences from the previous case are small and hard to see.

The feedforward control variables are shown in Figure 5e. Note that these variables are the same as the first case simulations for the same reasons discussed previously; i.e., the pilot input commands are the same, the command model and the plant model used in the feedforward control design are the same as the first case.

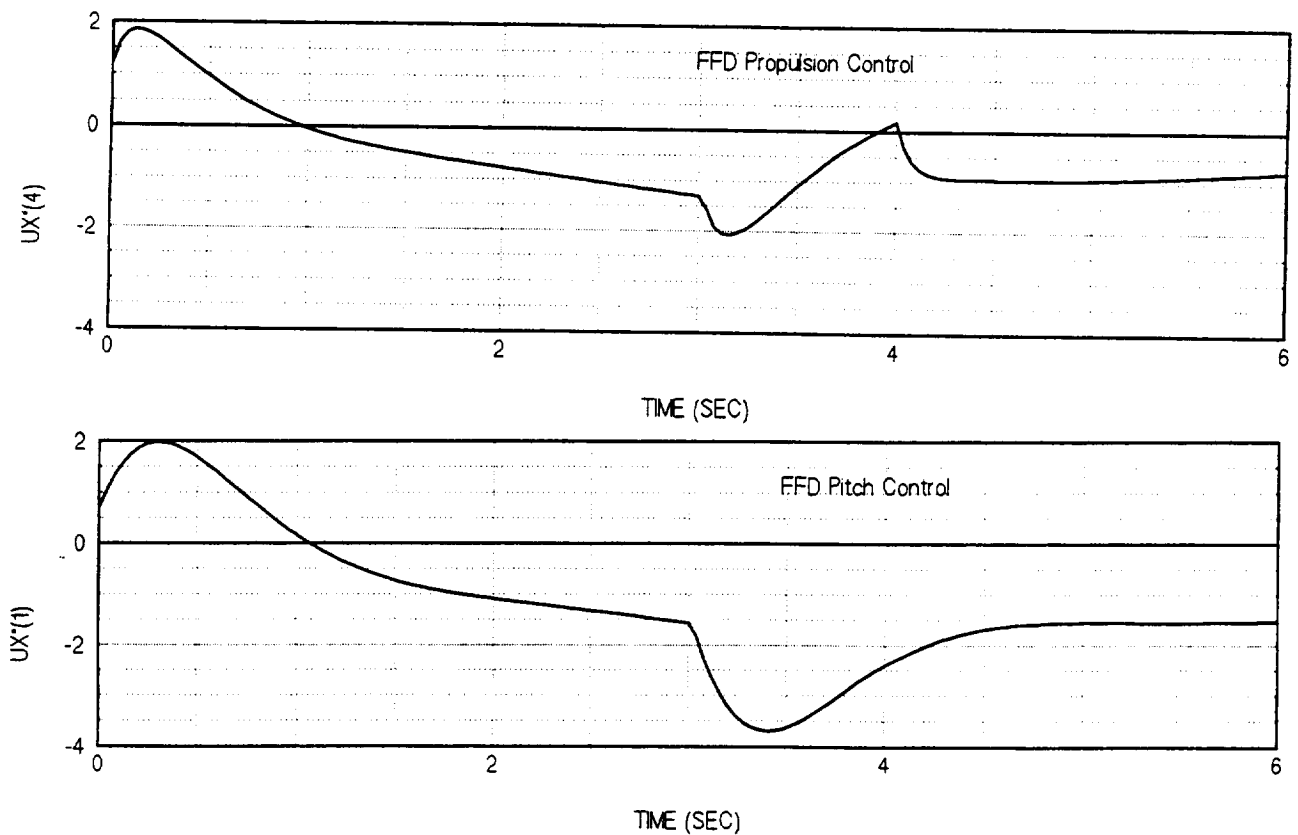


Figure 5e. Modified F-15 SMTD Integrated SOFFT Control Simulation, Perturbed Plant Feedforward Control Variables

The feedback control variables are shown in Figure 5f. Note that the feedback control law in this case is not null and is trying to reduce the errors present between the actual state and the feedforward state corresponding to the desired response. Thus, a 10% error in the control effectiveness matrix is barely noticed. It should also be noted that the feedback control is able to achieve this response with a control effort equal to approximately one tenth of the feedforward control levels. Of course, when plant and measurement noise is present, the feedback control activity will increase noticeably as the high frequency content will increase.

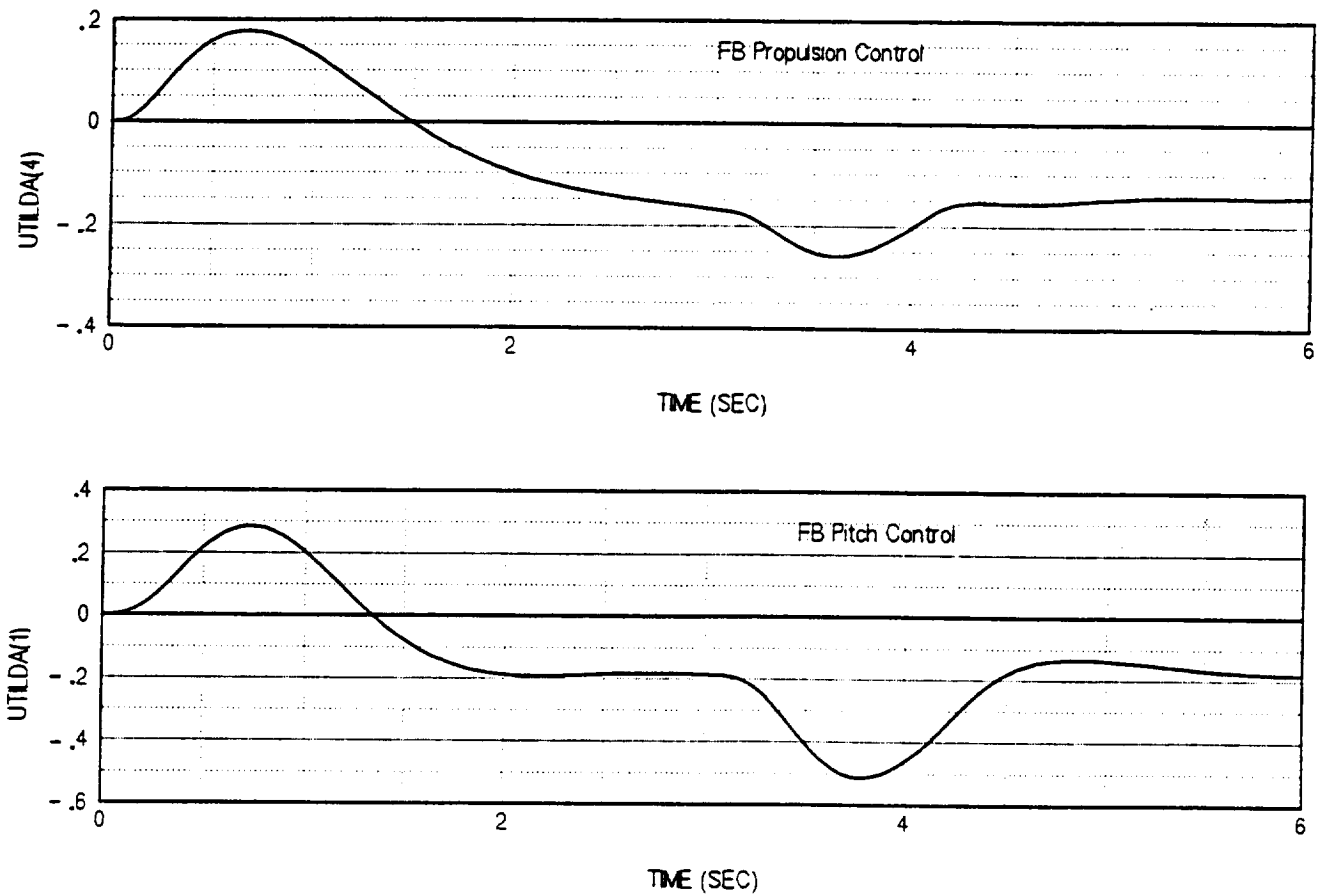


Figure 5f. Modified F-15 SMTD Integrated SOFFT Control Simulation, Perturbed Plant
Feedback Control Variables

The closed-loop modes of the aircraft are shown in Table 15.

Table 15. Closed-Loop Equivalent s-plane Eigenvalues

REAL	IMAGINARY	DAMPING RATIO	NATURAL FREQUENCY
-0.001793	0.000000	1.00	0.00
-0.016570	0.000000	1.00	0.02
-0.017264	0.000000	1.00	0.02
-0.101969	0.000000	1.00	0.10
-0.108535	0.000000	1.00	0.11
-0.392538	0.000000	1.00	0.39
-0.555280	0.000000	1.00	0.56
-1.986110	-2.050269	0.70	2.85
-1.986110	2.050269	0.70	2.85
-2.289180	-0.513772	0.98	2.35
-2.289180	0.513772	0.98	2.35
-2.359946	-0.092281	1.00	2.36
-2.359946	0.092281	1.00	2.36
-4.524391	-4.666417	0.70	6.50
-4.524391	4.666417	0.70	6.50
-6.218162	-4.595787	0.80	7.73
-6.218162	4.595787	0.80	7.73
-10.174557	0.000000	1.00	10.17
-12.552118	0.000000	1.00	12.55
-56.438641	0.000000	1.00	56.44
-199.904281	0.000000	1.00	199.90

V. CONCLUSIONS

The need for integrated or constrained control systems came into greater focus as advanced aircraft brought new subsystems with significant coupling between them. These included advanced propulsion subsystems with vectored thrust and new aerodynamic designs of the airframe sometimes with new surfaces such as canards and sometimes with fewer control surfaces such as the tailless aircraft. The coupling produced by these subsystem developments only added to the existing need for a general method for designing control laws with arbitrary coupling constraints for decentralized systems.

In this study, we develop an integrated control design methodology which accommodates constraints on the coupling of subsystems or variables. The methodology uses the SOFFT control approach and structure, thus maintaining all the advantages of the SOFFT approach.

The Integrated/Constrained SOFFT Control methodology uses a centralized feedforward control and a constrained feedback control law. The main conclusion of this work is that the approach mentioned takes advantage of the coupling among the various subsystems while maintaining the identity of subsystems for validation purposes and the simplicity of the feedback control law for ease of understanding the system's behaviour in complicated nonlinear scenarios. While the use of a centralized SOFFT feedforward is recommended, it is not a necessity for the methodology. It is possible to use a constrained SOFFT feedforward to accommodate constraints using the algorithm developed for feedback systems or by using other methods. The methodology is formulated in detail and the necessary mathematical development is shown in the previous sections.

The Variable-Gain Output Feedback Control methodology is extended to include equality constraints which can avoid coupling two variables or two subsystems. Although this approach was developed within the SOFFT context, it is an independent method for

designing feedback control laws which can be used with or without any feedforward control system. The Variable-Gain Output Feedback Algorithm is extended to accommodate equality constraints by specifying that any element of the gain matrix be zero.

In a more general setting, the algorithm developed can have nonzero values placed as constraints as well. This allows the optimization of one part of a control law while the other part (which may have been designed and tested under previous circumstances) is left unchanged. Another application is to produce a known amount of coupling between two variables, such as the aileron-rudder interconnect, by constraining a gain element or block to maintain a specified value while optimizing the remaining control gains. The algorithm is monotonic in the cost, reducing the cost at each iteration. The rate of convergence depends on the particular problem and on the particular constraints placed for a given problem.

Finally, the Integrated SOFFT Control methodology is used to design an integrated flight and propulsion control system for the modified F-15 SMTD aircraft as an example of the approach developed. A centralized SOFFT feedforward control law and a constrained output feedback control law are designed at a 30 degree angle-of-attack flight condition. Using the SOFFT approach, the command model is selected to produce desirable flying qualities for the aircraft. The response of the aircraft to some pilot input commands are presented.

REFERENCES

1. Halyo, N., Direskeneli, H. and D. B. Taylor, "A Stochastic Optimal Feedforward and Feedback Control Methodology for Superagility", NASA CR-4471, November 1992
2. Halyo, N., "A Stochastic Optimal Feedforward and Feedback Control Methodology for Superagility", ICS FR-689102, Information & Control Systems, Inc., 732 Thimble Shoals Blvd., Newport News, VA, 1989.
3. Halyo, N. and J. R. Broussard, "Investigation, Development, and Application of Optimal feedback Theory. Volume I ---A Convergent Algorithm for the Stochastic Infinite-Time Discrete Optimal Output Feedback Problem", NASA CR-3828, August 1984
4. Halyo, N. and R. E. Foulkes, "On the Quadratic Sampled-Data Regulator with Unstable Random Disturbances", *IEEE SMC Cos. Proc. 1974 Int. Conf. on Sys., Man and Cybern.*, October 1974.
5. Halyo, N., Moerder, D. D., Broussard, J. R. and D. B. Taylor, "A Variable-Gain Output Feedback Control Design Methodology", NASA CR-4226, March 1989.
6. Halyo, N., "A Variable-Gain Output Feedback Control Design Approach", *Proc. AIAA Guidance Navigation, and Control Conf.*, Boston, MA, August 1989.
7. Halyo, N. and J. R. Broussard, "A Convergent Algorithm for the Stochastic Infinite-Time Discrete Optimal Output Feedback Problem", *Proc. of the 1981 Joint Auto. Control Conf.*, Volume 1., Amer. Auto. Control Council, c. 1981, paper WA-1E. Charlottesville, VA.
8. Ostroff, A. J., "High-Alpha Application of Variable-Gain Output Feedback Control", *J., Guidance, Control and Dynamics*, Vol. 15, No. 2, pp. 491-497, March-April 1992.

9. Hueschen, R. M., "The Design, Development, and Flight Testing of a Modern Control-Designed Autoland System", *American Control Conference*, Boston, MA, June 1985.
10. Halyo, N. and A. K. Caglayan, "A Separation Theorem for the Stochastic Sampled-Data LQG Problem", *Int. J. Control*, Volume 23, No. 2, pp. 237-244, February 1976.
11. R. E. Kalman and R. S. Bucy (1961), "New Results in Linear Filtering and Prediction Theory", *J. Basic Eng., Trans. ASME*, Ser. D, 83, pp. 95-108.
12. Kwakernaak, H. and R. Sivan, *Linear Optimal Control Systems*, John Wiley & Sons, Inc., New York, 1972.
13. Broussard, J. R. and C. S. McLean, "An Algorithm for Simultaneous Stabilization Using Decentralized Constant Gain Output Feedback", *IEEE Trans. on Automatic Control*, Vol. 38, No. 3, pp. 450-455, March 1993.
14. Etkin, B., *Dynamics of Atmospheric Flight*, John Wiley & Sons, Inc., New York, 1972.

APPENDIX A

INCREMENTAL IMPLEMENTATION WITH CONTROL RATE LIMITS

The incremental implementation given in [5], pp.46-50, can be used to implement the SOFFT control laws developed in this work. However, this implementation is intended for systems with position limiters placed on the control values. Here, we want to present an incremental implementation for systems which contain both control position and control rate limiters.

The motivation for using an incremental implementation rather than a standard implementation (which would use total values) remains essentially the same; i.e., avoiding integrator wind-up due to position limiters, eliminating the use of trim values, improving the response to constant disturbances, etc. In the present implementation, **we include the effect of control rate limiters on tracking errors and the resulting introduction of phase shifts or time delays which can produce significant instabilities in the closed-loop system.** The reasons for selecting one particular form of incrementation over another are of a heuristic nature. Here, we simply present the proposed incremental implementation without further comment.

The system we want to control is of the form shown in eq. (81) and (82) or , more generally, as given in [5], eq. (22) and (23). These represent a nonlinear system having a wide operating range over which the system parameters may vary considerably. The details of the linearization are shown in Section II.1 of [5].

Compute the control position command using the following equations.

$$u_{xk} = \lim_p \{ u_{xk-1} + \Delta t v_k \} \quad (\text{A-1})$$

$$v_k = \lim_R \{ v_{k-1} + \Delta \tilde{v}_{k-1} + (\Delta u_{xk}^* - \Delta u_{xk-1}^*) / \Delta t \} \quad (\text{A-2})$$

where \lim_R and \lim_p are functions which limit the control rate and the control position to the specified range of values, respectively. We select these limits to be the same as those set by the plant actuator limiters. In other words, the system actuators do not allow the control position and rate to go above these values. Accordingly, **the performance of the closed loop plant is not impacted by the software limit functions** placed in the equations above, at least not immediately.

The feedforward control law can be implemented as follows.

$$z_{k+1} = \Phi_z(p_k) z_k + \Gamma_z(p_k) u_{xk} \quad (\text{A-3})$$

$$\Delta z_k = z_k - z_{k-1} \quad (\text{A-4})$$

$$\Delta u_{xk} = u_{xk} - u_{xk-1} \quad (\text{A-5})$$

$$\Delta u_{xk}^* = -K_x^*(p_k) \Delta x_k^* - K_z(p_k) \Delta z_k - K_{uz}(p_k) \Delta u_{xk} \quad (\text{A-6})$$

$$\Delta x_{k+1}^* = \Phi_x(p_k) \Delta x_k^* + \Gamma_x(p_k) \Delta u_{xk}^* \quad (\text{A-7})$$

$$\Delta y_{xk}^* = C_x(p_k) \Delta x_k^* \quad (\text{A-8})$$

$$y_{xk}^* = y_{xk-1}^* + \Delta y_{xk}^* \quad (\text{A-9})$$

We do not place any limiters on the feedforward control variables computed in the above equations. However, depending on the particular problem, it may be necessary or desirable to place some limits on the feedforward state, measurement or control variables.

Also note that the total value of the feedforward state vector is not computed although a value is implied by the incremental feedforward state vector which is used to compute the total value (except for the measurement bias value which will cancel out in (A-11)) of the feedforward measurements. Similarly, the total value of the feedforward control is not computed in this implementation.

The feedback control law is implemented as follows.

$$\tilde{y}_{xk} = y_{xk} - y_{xk}^* \quad (A-10)$$

$$\Delta \tilde{y}_{xk} = \tilde{y}_{xk} - \tilde{y}_{xk-1} \quad (A-11)$$

$$\begin{aligned} \Delta \tilde{v}_k = & -K_x(p_k) \Delta \tilde{y}_{xk} - \Delta t K_I(p_k) \left[H_y(p_k) \tilde{y}_{xk-1} + H_u(p_k) \tilde{u}_{xk-1} \right] \\ & - \Delta t K_v(p_k) \tilde{v}_{k-1} \end{aligned} \quad (A-12)$$

$$\tilde{v}_k = \tilde{v}_{k-1} + \Delta \tilde{v}_k \quad (A-13)$$

$$\tilde{u}_{xk} = \tilde{u}_{xk-1} + \Delta t \tilde{v}_{k-1} \quad (A-14)$$

We do not place any limiters on the feedback state, measurement or control vectors in the equations above although circumstances may necessitate their use in certain problems. The limiting function is placed on the total control rate and control position vectors shown in equations (A-1) and (A-2). In a sequential presentation of the incremental implementation equations, first (A-2) then (A-1) would follow (A-14).

It is also important to note that the control filtering action of the PIF feedback structure is still present in the implementation given above. Equation (A-12) is simply an algebraic restatement of the more usual form of this equation. As long as no limits are placed on the feedback implementation equations, the filtering action will be present.

APPENDIX B

INTEGRATED FLIGHT AND PROPULSION MODEL DERIVATION

In this appendix, we show the derivation of the integrated flight and propulsion model used in Section IV.A. as the example problem which is a modified version of the F-15 SMTD aircraft. The derivation is quite straight-forward and is given here for completeness.

The state equations for the airframe and propulsion subsystems are of the form

$$\dot{x}_1 = A_1 x_1 + B_1 u_{x1} + B'_{11} u_{11} \quad (\text{B-1})$$

$$\dot{x}_2 = A_2 x_2 + B_2 u_{x2} + B'_{22} u_{22} \quad (\text{B-2})$$

where the subscript 1 denotes the airframe parameters and the subscript 2 denotes the propulsion parameters. The cross-coupling terms, the last terms in the equations above, are given by

$$u_{11} = \begin{pmatrix} F_g \\ D_p \end{pmatrix} \quad u_{22} = \begin{pmatrix} \alpha \\ \beta \end{pmatrix} \quad (\text{B-3})$$

where F_g and D_p are the gross thrust and the drag due to the engine.

The cross-coupling terms defined above can be expressed in terms of the state and control vectors as follows.

$$u_{11} = E_{12}x_2 + F_{12}u_{x2} + G_{12}u_{z2} \quad (\text{B-4})$$

$$u_{z2} = E_{21}x_1 \quad (\text{B-5})$$

Since the airframe model includes both the longitudinal and lateral dynamics, the components of u_{z2} , namely the angle-of-attack and the sideslip angle, can be expressed in terms of the airframe state alone.

Substituting (B-5) into (B-4), eliminate the cross-coupling term u_{z2} .

$$u_{11} = (G_{12}E_{21})x_1 + E_{12}x_2 + F_{12}u_{x2} \quad (\text{B-6})$$

$$= E_{11}x_1 + E_{12}x_2 + F_{12}u_{x2} \quad (\text{B-7})$$

Now substituting (B-5) and (B-7) for the cross-coupling terms in (B-1) and (B-2) and manipulating, the integrated continuous open-loop system can be found as

$$\dot{x}_1 = [A_1 + B'_{11}E_{11}]x_1 + [B'_{11}E_{12}]x_2 + B_1 u_{x1} + [B'_{11}F_{12}]u_{x2} \quad (\text{B-8})$$

$$\dot{x}_2 = [B'_{z2}E_{21}]x_1 + A_2 x_2 + B_2 u_{x2} \quad (\text{B-9})$$

Comparing (116) and (117) with (B-8) and (B-9), we note that they have the same form. Therefore, equating the system matrices provides the desired result.

REPORT DOCUMENTATION PAGE			Form Approved OMB No. 0704-0188	
Public reporting burden for this collection of information is estimated to average 1 hour per response, including the time for reviewing instructions, searching existing data sources, gathering and maintaining the data needed, and completing and reviewing the collection of information. Send comments regarding this burden estimate or any other aspect of this collection of information, including suggestions for reducing this burden, to Washington Headquarters Services, Directorate for Information Operations and Reports, 1215 Jefferson Davis Highway, Suite 1204, Arlington, VA 22202-4302, and to the Office of Management and Budget, Paperwork Reduction Project (0704-0188), Washington, DC 20503.				
1. AGENCY USE ONLY (Leave blank)		2. REPORT DATE July 1996		3. REPORT TYPE AND DATES COVERED Contractor Report
4. TITLE AND SUBTITLE Integrated Control Using the SOFFT Control Structure			5. FUNDING NUMBERS C NAS1-20185 WU 505-68-33-01	
6. AUTHOR(S) Nesim Halyo				
7. PERFORMING ORGANIZATION NAME(S) AND ADDRESS(ES) Information & Control Systems, Inc. 732 Thimble Shoals Blvd., Suite 801 Newport News, VA 23606			8. PERFORMING ORGANIZATION REPORT NUMBER	
9. SPONSORING / MONITORING AGENCY NAME(S) AND ADDRESS(ES) National Aeronautics and Space Administration Langley Research Center Hampton, VA 23681-0001			10. SPONSORING / MONITORING AGENCY REPORT NUMBER NASA CR-4748	
11. SUPPLEMENTARY NOTES Langley Technical Monitor: A. J. Ostroff				
12a. DISTRIBUTION / AVAILABILITY STATEMENT Unclassified Unlimited Subject Category - 08			12b. DISTRIBUTION CODE	
13. ABSTRACT (Maximum 200 words) The need for integrated/constrained control systems has become clearer as advanced aircraft introduced new coupled subsystems such as new propulsion subsystems with thrust vectoring and new aerodynamic designs. In this study, we develop an integrated control design methodology which accomodates constraints among subsystem variables while using the Stochastic Optimal Feedforward/Feedback Control Technique (SOFFT) thus maintaining all the advantages of the SOFFT approach. The Integrated SOFFT Control methodology uses a centralized feedforward control and a constrained feedback control law. The control thus takes advantage of the known coupling among the subsystems while maintaining the identity of subsystems for validation purposes and the simplicity of the feedback law to understand the system response in complicated nonlinear scenarios. The Variable-Gain Output Feedback Control methodology (including constant gain output feedback) is extended to accomodate equality constraints. A gain computation algorithm is developed. The designer can set the cross-gains between two variables or subsystems to zero or another value and optimize the remaining gains subject to the constraint. An integrated control law is designed for a modified F-15 SMTD aircraft model with coupled airframe and propulsion subsystems using the Integrated SOFFT Control methodology to produce a set of desired flying qualities.				
14. SUBJECT TERMS Feedforward, Feedback, SOFFT, Integrated, Control, Optimal, Constrained, Output feedback, Flight & propulsion			15. NUMBER OF PAGES 98	
			16. PRICE CODE A05	
17. SECURITY CLASSIFICATION OF REPORT Unclassified	18. SECURITY CLASSIFICATION OF THIS PAGE Unclassified	19. SECURITY CLASSIFICATION OF ABSTRACT	20. LIMITATION OF ABSTRACT	